Hontomin reservoir characterisation tests

Final technical report

JUNE 2015

Authors:

G.Ortiz, T.Kovacs, Daniel .F. Poulussen and C.de Dios

CIUDEN

Collaborators:

L. Martinez-Landa, J. Carrera, L.J., Slooten, S. De Simone, J. Soler, B. Gomez and S. Fernández

Ground Water Hydrology Group of UPC-CSIC Barcelona

Summary

The Hontomín site (Burgos province, North Central Spain) hosts the Technological Development Plant (TDP) for CO_2 geological storage associated with the Compostilla project OXYCFB300, operated by "Fundación Ciudad de la Energía" (CIUDEN). This report has been prepared by CIUDEN on behalf of the Global CCS Institute, to describe reservoir characterization activities undertaken at the site.

The storage complex is located in lower Jurassic formations at 1.5 km depth: marls as the upper seal, limestones and dolomites as the storage formation, and anhydrites as the lower seal. As part of the TDP, two wells have been drilled: H-I (CO_2 injection well) and H-A (observation well).

CO_2 will be injected into fractured carbonate rocks of relatively low permeability. As CO_2 rich brine may dissolve carbonates, reservoir integrity could be affected by high dissolution around or in the vicinity of the injection well depending on the local flow rate conditions. Due to the fractured nature of the formation, it is essential to conduct a detailed study of the structural geology to identify the main fractures and the stress distribution. The existence of fractures within the reservoir increases the secondary porosity and permeability, and thus increases CO_2 injectivity into the reservoir.

In order to assess the hydraulic properties and geochemical reactivity of the storage reservoir, significant efforts have been devoted to characterization prior to CO_2 injection. In order to obtain an initial estimate of the permeability of the storage formation immediately after drilling, a preliminary hydraulic characterization campaign was carried out. Brine injection tests were performed in both the injection and the monitoring wells. Pressure, temperature and flow rates were recorded during these tests. Micro-seismicity was measured with an accelerometer located on the injection site.

Several tests were performed by changing the flow-rate and injection time, in order to assess the behaviour of the aquifer at different pressure conditions.

Interpretation of these tests was complicated by several factors. Firstly, it has been necessary to analyse injections and recoveries separately due to the different behaviour of the reservoir during these periods. If the reservoir had not been affected by mechanical factors, the increase in flowrate should have been proportional to the increase in pressure. However, increased pressures were lower than expected for the corresponding increase in flowrate. The transmissivity results obtained from the injection period should have been equal to that obtained during the post-injection recovery period;. However, much higher transmissivity values were observed during the injection than during recovery.

The pressure evolution indicated that water flows sequentially through a skin and into the fracture network. When pressure build-up reached a sufficient level, fractures in the formation may have widened or opened, increasing transmissivity. When injection was stopped, initial measurements were consistent with the previously observed flow behaviour; however, subsequently pressure increases indicated a drop in transmissivity which may be interpreted as closure of the fractures.

The tests were interpreted using a conventional code (TRANSIN) and a code that allows changing transmissivity values during time (PROOST). The results obtained with these interpretations show that it is possible fit all collected data during injection and recovery (post-injection) periods of the tests.

These changes of transmissivity with variations in pressures were related to mechanical effects and elastic in nature, since transmissivity returned to its prior values once pressure dropped. This behaviour will be accounted for in the development of future injection strategies, and is why it is necessary to perform hydro-mechanical (HM) modelling to account the variations in reservoir transmissivity. It should be emphasized that the aim of the HM simulations was to explain the general behavior of the aquifer during the injection tests; quantitative calibration was limited by the difficulty in matching simulations to observed data, especially in the recovery period.

The dependence of transmissivity on the injection regime will be important in subsequent characterization tests, CO_2 storage experiments and modeling efforts. For design purposes and based on the work described in this report, the following value conclusions have been drawn.

In well HA, transmissivity varied between 0.003m^2/d (which corresponds to a permeability of 0.015mD for the formation thickness of 165m) at low pressures and 0.04m^2/d (which corresponds to a permeability of 0.19mD) at high pressures. The well displayed a significant skin effect.

In well HI, transmissivity varied between 0.02m^2/d (which corresponds to a permeability of 0.12mD for the formation thickness of 133m) at low pressures and 0.3m^2/d (or 1.8mD) at high pressures (flow rate of 3L/s, and overpressure of 70bar at the well head). Skin effects observed during the first injections disappeared in later tests.

Subsequent characterization tests carried out at Hontomin indicated notable increases in reservoir permeability, up to four times the original value. Nevertheless, these tests are part of a protocol which is following a process to be patented, so limited information can be provided. They are mainly related to a set of injection tests using brine and/or CO2. Transmissivity values acquired during this process are over 100mD*m, with a parallel modeling effort that keeps reactive and hydrodynamic features into account. This underlines the need for thorough characterization of CO_2 storage sites in order to acquire a better understanding of the processes that will take place during operations.

TABLE OF CONTENTS

1 INTRODUCTION

1.1 MOTIVATION AND OBJECTIVES

The lifecycle of a CO_2 storage site includes several phases, from project screening to site closure. A key phase is site characterization, critical for the definition of a specific site for CO_2 storage that fulfils the criteria of containment, capacity and injectivity.

Site characterization may be defined as "the collection, analysis and interpretation of subsurface, surface and atmospheric data (geoscientific, spatial, engineering, social, economic, environmental) and the application of that knowledge to judge, with a degree of confidence, if an identified site will geologically store a specific quantity of CO_2 for a defined period of time and meet all required health, safety, environmental and regulatory standards" (Cook, 2006). Geological, geochemical, hydrogeological and geomechanical data should be taken into account for the assessment of capacity, containment and injectivity.

Storage capacity evaluates the available pore volume for CO_2 storage in a particular site. It is controlled by parameters such as the size of the containment area, the thickness of the reservoir, the effective porosity and the density of the CO_2.

Containment may be defined as the retention of injected CO_2 within the subsurface site relative to the overall risks of its escape. Containment is an issue in CO_2 storage because injected supercritical CO_2 is less dense than water and has the tendency to be driven upward due to buoyancy forces (CO2CRC, 2008). One of the issues involving containment is reservoir and seal integrity (rock strength, fault/fracture stability and maximum sustainable pore fluid pressures).

Injectivity may be defined as the rate at which CO_2 can be injected into a given reservoir interval and the ability of the subsequent CO_2 plume to migrate away from the injection well. Injectivity issues that can be analyzed through characterization activities include the geometry and connectivity of individual flow units, the nature of the heterogeneity within those units and the physical quality of the reservoir in terms of porosity and permeability characteristics (CO2CRC, 2008).

In spite of the development of several sites for CO_2 storage in the last 20 years, and the publication of some valuable reference documents as the "Best Practices for Site Screening, Site Selection, and Initial Characterization" from the US DOE or the "Best Practices Manual from SACS (Saline Aquifer CO_2 Storage Project) for Storage of CO_2 in Deep Geologic Formations", no standard methodology has been established for site characterization. This report aims to show the advances in reservoir characterization made from the work undertaken at Hontomin.

CO_2 Storage has reached significant scale (1Mt+ CO_2) in sites such as Sleipner, In-Salah and Decatur. Other CO_2 injection operations at smaller scale (typically <0.1Mt CO_2) have also achieved notable results, including Otway, Ketzin, Nagaoka, Lacq and examples within the Regional Carbon Sequestration Partnership of the Department of Energy in the US. The Hontomin site has been designed to operate at a similar pilot scale.

All these sites have provided valuable information and experience under different conditions, including shallow reservoirs (Ketzin), very deep ones (Lacq), or facing earthquakes (Nagaoka).

The Hontomin site represents an opportunity to develop injection and CO_2 storage-related activities in a low permeability, carbonate deep saline aquifer – which is a novel approach for dedicated geological storage, and could provide learnings for potential storage operations in other 'less than ideal' sites. It should be noted that considerable experience of CO_2 injection into relatively low permeability carbonates has been gained through enhanced oil recovery (CO2-EOR) operations in North America, for example at Weyburn in Canada (Wildgust et al, 2013)...

After the collection and interpretation of all available data, drilling of the two wells took place at Hontomin in 2013. Once drilling works were completed, a set of hydraulic tests was performed in each well, for the purpose of characterizing the reservoir (transmissivity values), leading to a better definition of parameters related to containment, injectivity, and informing future injection approaches at this experimental test site.

Injection tests with brine were then undertaken to validate field permeability and identify any barriers to the required injection rates and pressures in the reservoir. These tests also provided an opportunity to study interference and pressure pulses between the two wells.

Once brine injection and connectivity tests were undertaken and analyzed, further hydraulic testing was carried out to check the reservoir response under different regimes (Fig. 1.1).

The objective of this report is provide a detailed interpretation of the preliminary hydraulic tests and an analysis of the results to inform further characterization work, including future CO_2 injection tests.

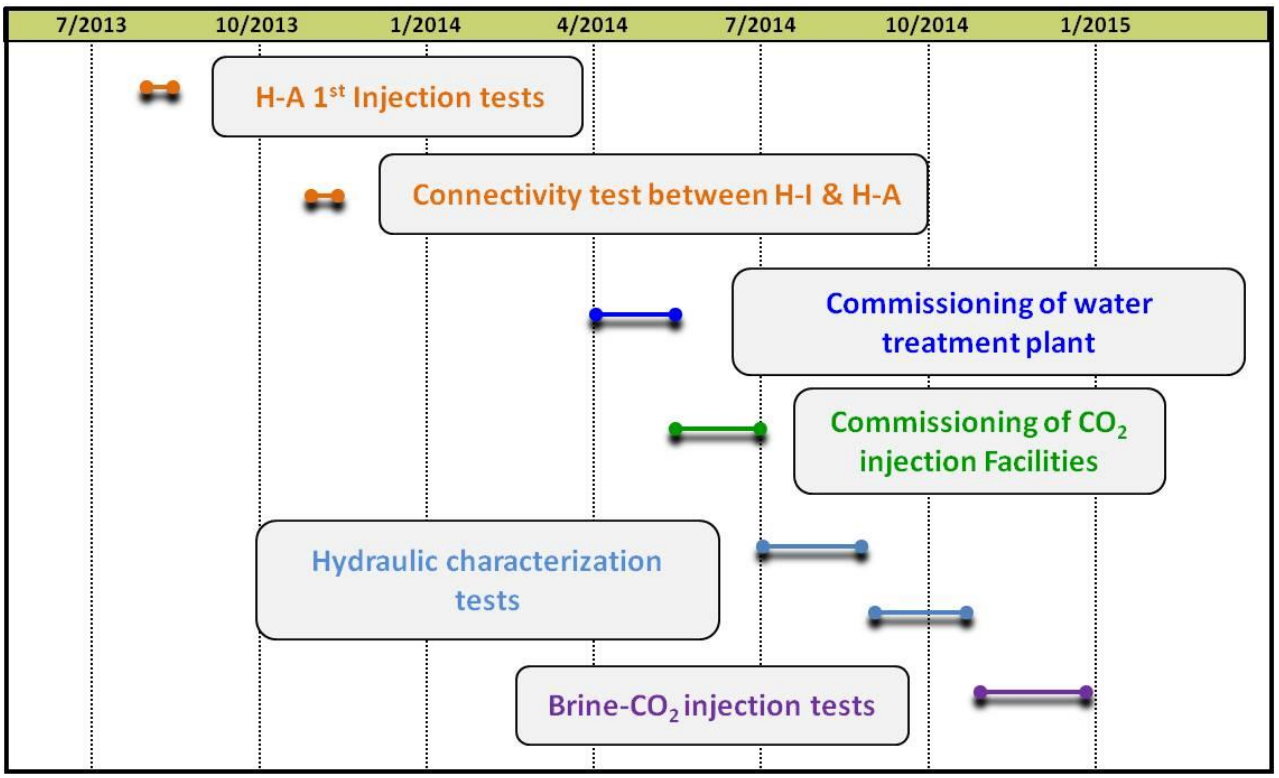

Fig. 1.1 Timeline including the tests performed at Hontomin. Tests explained in this report are highlighted in orange.

2 THE HONTOMÍN SITE

The Hontomín site (Figure 2.1) is located in the province of Burgos in North Central Spain and hosts the Technological Development Plant (TDP) for CO_2 geological storage within the Compostilla project OXYCFB300 operated by "Fundación Ciudad de la Energía" (CIUDEN). The Compostilla project comprises two phases: the first (Technology Development) involved the design, construction and operation of three independent facilities for CO_2 capture, transport and storage. The first two are located in the village of Cubillos del Sil (Leon), close to the existing Compostilla power plant; whereas the Hontomin CO_2 Storage Technology Development Plant (TDP) is located 250km eastwards. The second phase of the project, where

the commercial integrated project was supposed to enter into operation lead by Endesa at a site 130km east of Compostilla, has been postponed.

The geological setting of Hontomín consists of a dome-like structure located in formations of Lower Jurassic age: marls as the upper seal, limestones and dolomites as the storage formation, and anhydrites as the lower seal. The CO_2 will be injected into the carbonates located between approximately 1,440 and 1,570 m depth.

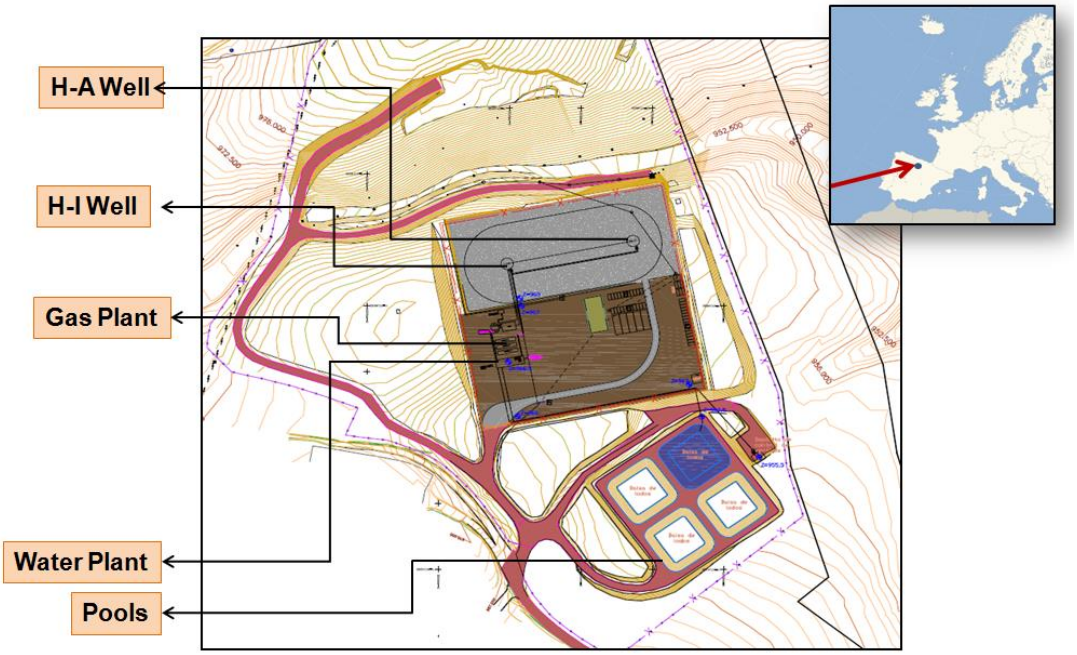

Figure 2.1: The Hontomín Site schematic view and location

As part of the TDP, two wells have been drilled: H-I (CO_2 injection well) and H-A (monitoring well). A number of CO_2 injection tests are planned at the site including supercritical and pulsating injection.

Both wells are fully instrumented and further monitoring capabilities include a shallower hydrogeological monitoring network, and a set of surface 30 microseismic stations.

.

Figure 2.2: General view of Hontomin site and CO_2 injection well

2.1 GEOLOGICAL BACKGROUND

The TDP is located in Hontomín (Burgos, northern Spain). The Hontomín site borders with the Ubierna Fault (NW-SE direction) to the south-west, the Poza de la Sal salt dome to the north and the Ebro basin to the east (**Error! Reference source not found.**).

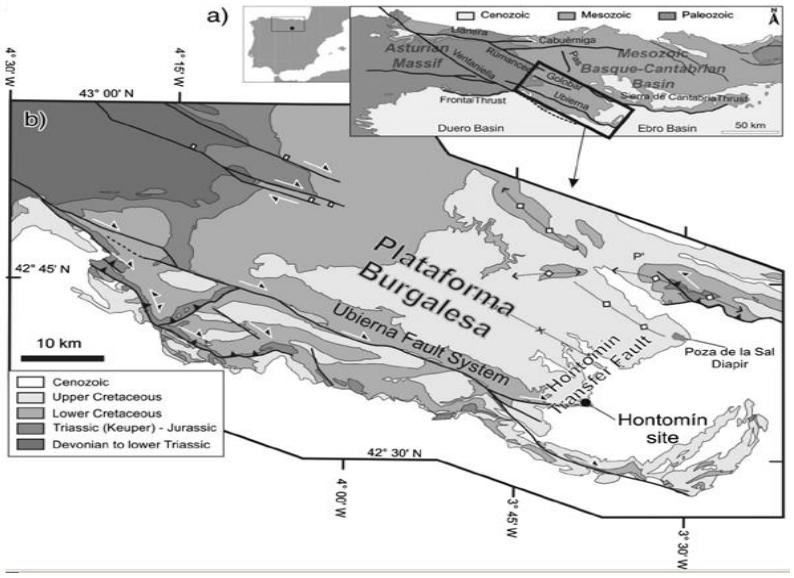

Figure 2.2: Simplified geological map showing the main geological features around Hontomín, bounded by Ubierna fault to the south-west, the Poza de la Sal salt dome to the north and the Ebro basin to the east (Alcalde et al., 2014)

From a geological perspective, Hontomín belongs to the Basque-Cantabrian Domain, north of the Ebro and Duero basins. It is part of the North Castilian Platform which was generated in the context of the opening of the North Atlantic and Bay of Biscay during Mesozoic times. During the Mesozoic extension, a thick sedimentary sequence was deposited in this area. Subsequently, the Alpine compression produced small-scale inversion structures which are detached along the Triassic evaporites. According to the available geological and geophysical data (2D seismic reflection images and borehole logs, borehole sample descriptions, etc.), the reservoir and seal formations are Jurassic in age and form a dome-like structure with an overall extent of 5 x 3 km (Figure. 2.3)

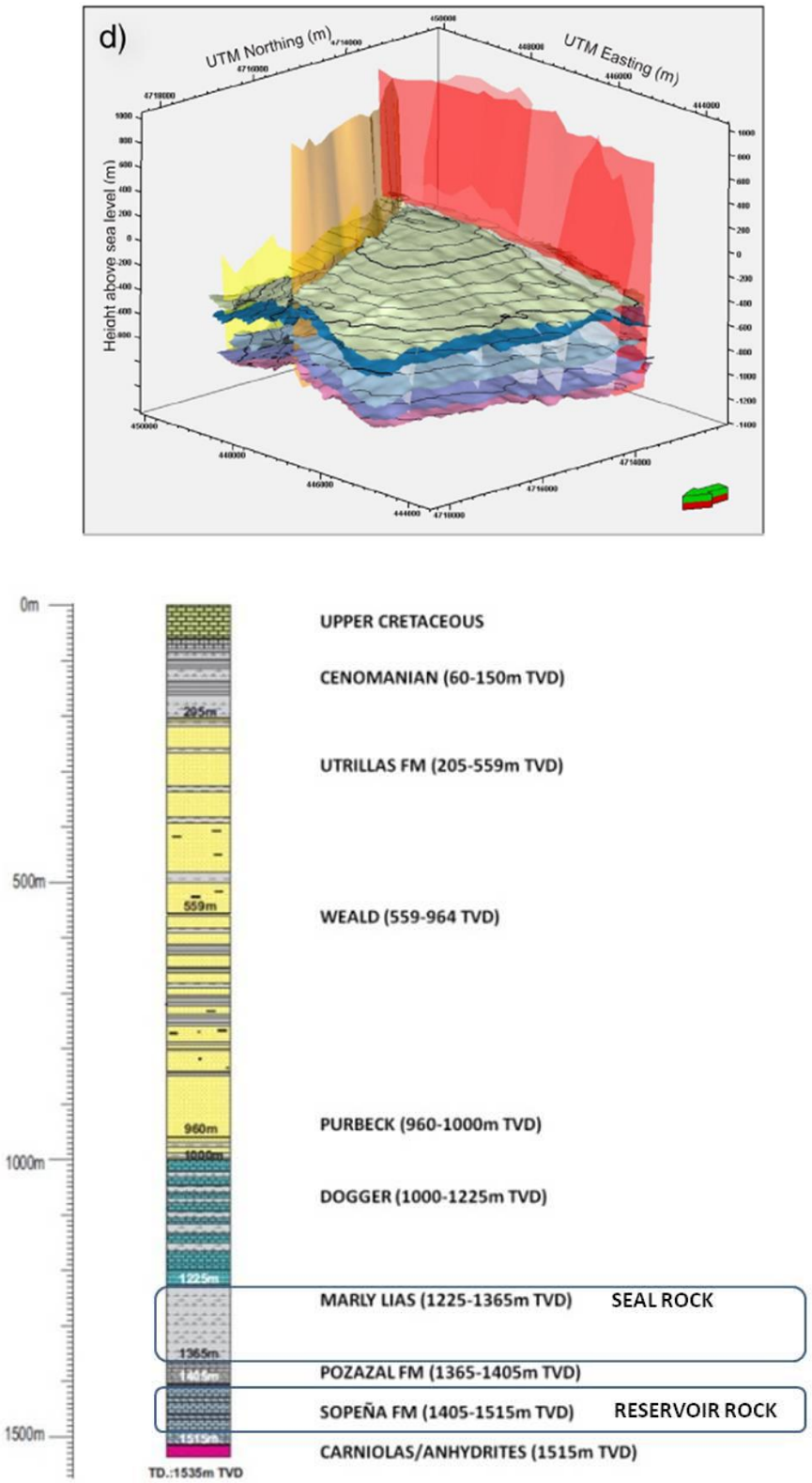

Figure 2.4: Top: Interpretation of the 3-D Hontomín dome structure dome with two main faults (Alcalde et al. 2014). Bottom: Stratigraphic column (Gessal)

The Mesozoic succession starts with Keuper Facies, which formed the core of the Hontomín dome. The Sopeña Fm is composed of evaporites, dolomites and marls, and overlies the Keuper Facies, forming the boundary between the Triassic and Lower Jurassic (Figure 2.4). The Lower Jurassic is constituted by deposits of a shallow marine carbonate ramp and the rest of the Jurassic succession was completed with carbonate and marls of a hemipelagic ramp. The Purbeck Facies of Upper Jurassic and Lower Cretaceous age (clays, sandstones and carbonate rocks) are placed unconformably on the top of the marine Jurassic rocks. The rest of the Lower Cretaceous is composed of Weald, Escucha, and Utrillas Facies which essentially are siliciclastic rocks. The rocks cropping out in the Hontomín area are carbonates of the Upper Cretaceous and the detritic and lacustrine Cenozoic rocks that lay unconformably over the Mesozoic succession.

The Hontomín structure is delimited by a normal fault to the north, which was active only during the Purbeck sedimentation. To the south, the structure is bounded by a strike slip fault associated with the Ubierna Fault.

Regional analysis has also been completed with the detailed study of outcrop samples and interpretation of the regional structures (Fig. 2.5).

Figure 2.5: Marls and black-shales (caprock) outcrop, 60km W-NW from Hontomín

The local geology has been further studied based on data obtained from the drilling of H-A and H-I boreholes, geological descriptions of the cuttings and cores and borehole logging (gamma, resistivity, caliper, acoustic televiewer, etc.). These studies confirmed the presence of the aforementioned stratigraphic sequence in the wells. The storage formation (Sopeña Fm.) was found to be of low primary porosity, with the reservoir capacity and permeability controlled by fracture-type (secondary) porosity. There is a continuous transition between the lower part of the reservoir (Dolomitic Sopeña Fm.) and the Keuper lower seal; this transition consists of the Carniolas unit. The main seal (Marly Lias Unit) overlays the Pozazal

formation, which is the transition between the reservoir and the caprock. This formation was found to have very low porosity and permeability values and thus can act as a secondary caprock.

2.2 THE HONTOMÍN TECHNOLOGY DEVELOPMENT PLANT

The Hontomin site offers reservoir conditions suitable for CO_2 injection in the liquid, gas or supercritical phases and is thus ideal for experimentation with different operational strategies. The CO_2 injection plant has three cryogenic injection pumps allowing injection rates between 0.5 and 2 kg/s and pressures over 80 bar, with three cryogenic CO_2 tanks of 50 ton capacity. The installation is completed with a gasifier to adjust the CO_2 temperature and a water injection plant, which plays a crucial role in pressure control during injection and other operational phases. The water injection plant includes a ceramic plunger pump capable of 120 bar pressure and 300 l/min flow injection, a 25000 l capacity deposit for water mixture preparations and two 2500 m^3 deposits for water storage besides the necessary water treatment equipment. The 1570 m deep injection and the monitoring wells are equipped with instrumentation ensuring the continuous monitoring of injection parameters, and a wide range of surface monitoring techniques are applied at the site for the assessment of injected CO_2 behaviour.

2.2.1 Injection well H-I

Injection well H-I was drilled between April and October 2013 with decreasing diameters ranging from 558.8 mm (22”) at ground level to 152.4 mm (6”) in the lowest section. The well has a total depth of 1,570 m and is cased down to a depth of 1,437 m; the casing shoe is located within Pozazal-Sopeña formations. The lowest 133 m of the well is open hole with a diameter of 152.4 mm, comprising the storage formation (calcareous and dolomitic Sopeña Formation) and part of the lower seal (Carniolas and Anhydrites formations). The injection interval was left as an openhole to facilitate study of the effects that CO_2 injection has on the reservoir. Well construction and instrumentation is shown in Figure 2.6.

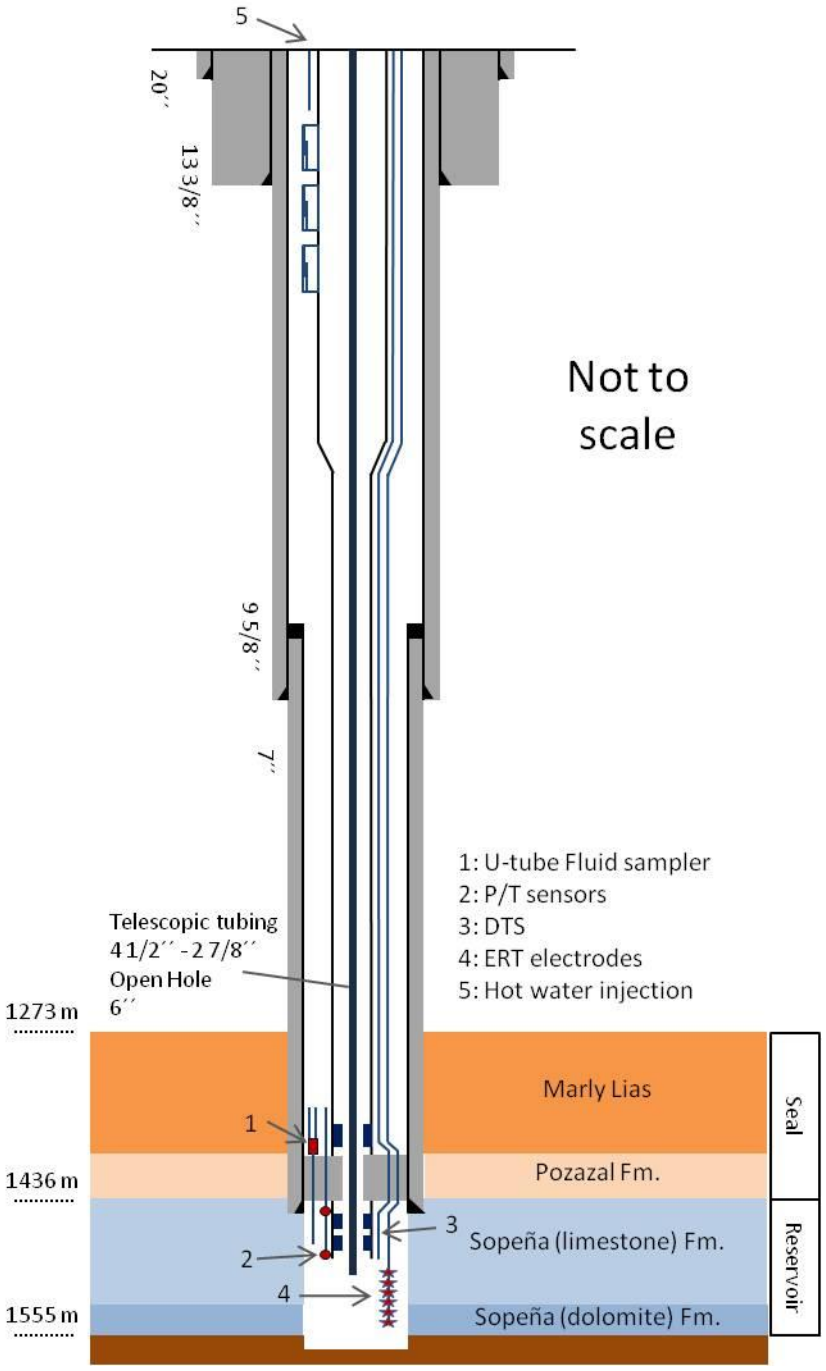

Figure 2.6: Structure of the injection well, H-I

2.2.2 Observation well H-A

The observation well H-A was drilled between April and July 2013 (completed before well H-I), with decreasing diameters ranging from 558.8 mm (22”) at ground level to 152.4 mm (6”) in the lowest section. The well has a total depth of 1,580 m and it is cased down to a depth of 1,281 m, the casing shoe being located within the Marly Lias. The lowest 299 m of the well are open hole with a diameter of 152.4 mm,

comprising part of the caprock (Marly Lias and Pozazal formations), the storage formation (calcareous and dolomitic Sopeña formations) and part of the lower seal (Carniolas and Anhidritas formations). The structure and instrumentation is shown in Figure 2.7.

.

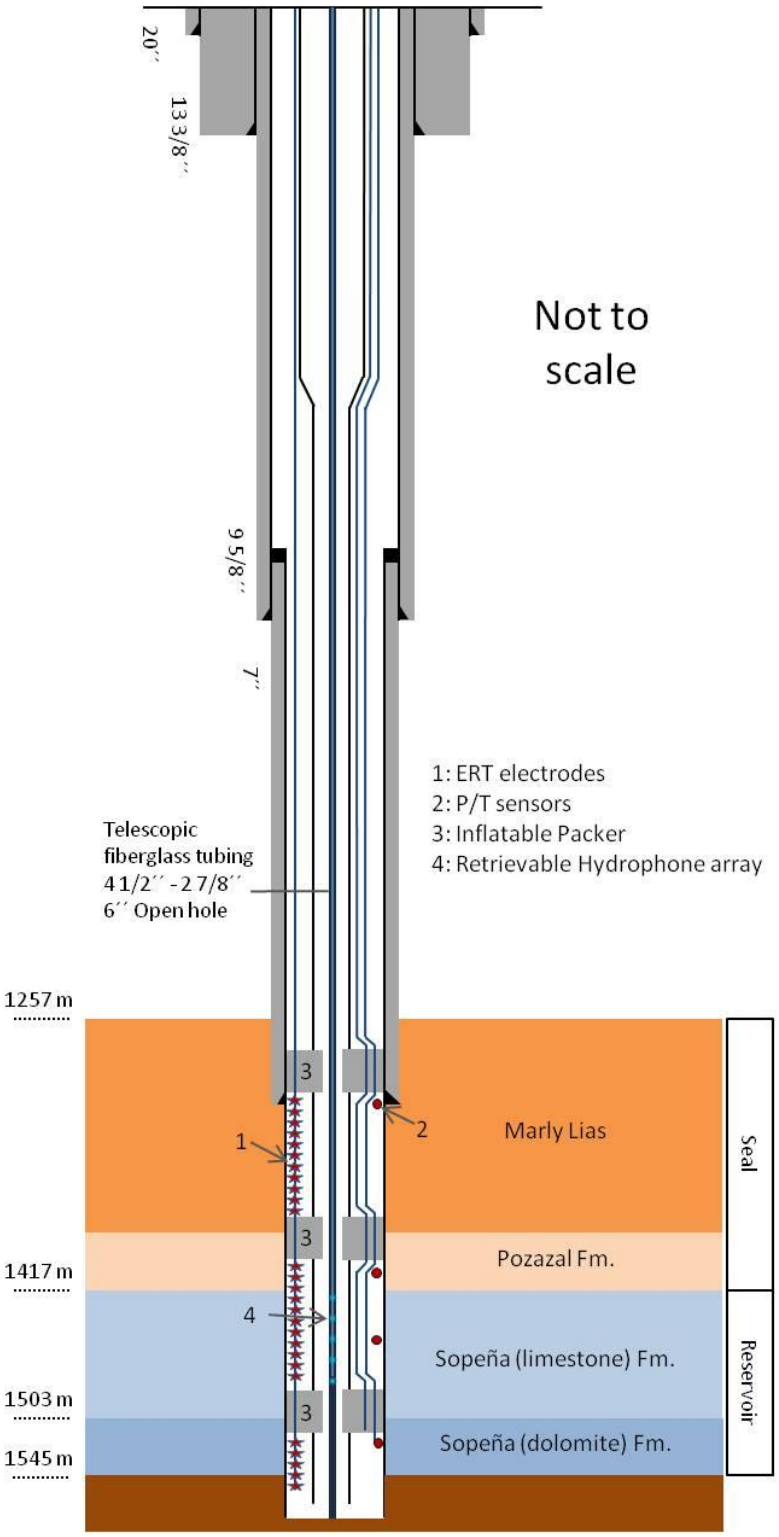

Figure 2.7: Structure of the monitoring well, H-A

3 METHODOLOGY

The methodology employed by the investigation comprised the following steps:

i. Hydraulic characterization tests in H-I and H-A wells:.

ii. Interpretation of hydraulic characterization tests with the following methods:

   - Filtering and de-trending of the data, calculation of drawdowns
   - Calibrating one by one each test individually to obtain a first estimate of hydraulic parameters during each test phase.
   - Interpretation of the complete series of hydraulic tests performed on each well using purely hydraulics models.
   - Interpretation of the complete series of hydraulic tests performed on each well using hydro-mechanical models.

It should be noted that a detailed understanding of the geological and geomechanical aspects of the reservoir is required to make sound interpretations of hydraulic testing.

4 HYDRAULIC CHARACTERIZATION TESTS

Hydraulic testing of the fractured carbonate reservoir at Hontomin has provided important information towards the design of CO2 injection operations. Such testing programs should allow characterization of the geomechanical properties of the reservoir and cap rock, monitor responses of the reservoir to injection, and assess any changes in permeability resulting from injection.

In order to obtain a first estimate of the permeability of the storage formation, a preliminary hydraulic characterization campaign was carried out immediately after the drilling of each of the two wells.

The observation well H-A was drilled first, and a preliminary interpretation of the brine injection tests performed upon completion in August 2013 revealed that:

i. The permeability of the storage formation in this well was lower than expected (less than 1mD). Low permeability could hinder both the planned characterization tests and the CO_2 injection phase.

ii. The measured permeability depended on the flow rate and overpressure applied during the tests. This indicated that fractures or fissures were opening upon pressurization of the borehole and closing again after the end of the brine injections.

Accordingly, well H-I was completed (November 2013) as open throughout the storage formation in order to obtain a better estimate of hydro-mechanical properties.

Figure 4.1 Field scene during the Hontomin characterization tests

4.1 HYDRAULIC TESTS ON H-A WELL

In August 2013, brine injection tests in the H-A well were carried out at Hontomin. A series of brine injection tests were performed at different positions along the length of the seal-reservoir system. **Error! Reference ource not found.**4.2 summarizes the main characteristics of the tests.

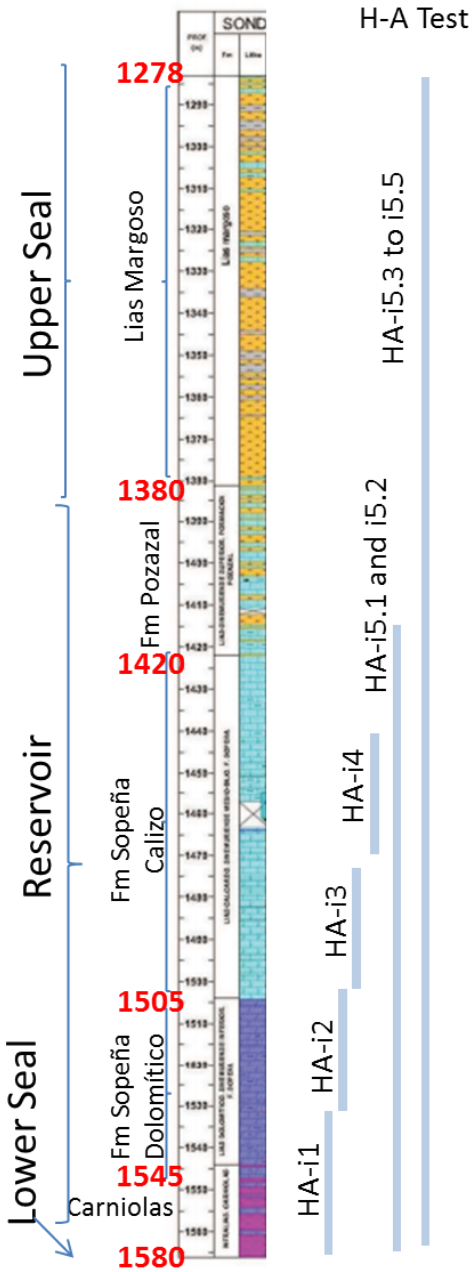

H-A Test

TEST	Interval Length (m)		DP (bar)	Q (l/min)	V_{Iny} (l)	t_{Iny} (min)
HA-i1	1530	1580	45.0	0.1	1.4	22.0
HA-i2	1501	1529.8	53.0	0.2	9.2	21.2
HA-i3	1472	1500.8	50.0	0.8	49.4	61.9
HA-i4	1439.1	1467.9	40.0	0.2	10.3	65.3
HA-i5-1	1414.2	1580	35.0	15.8	7.4	0.5
HA-i5-2			47.0	6.6	140.8	21.4
HA-i5-3	1283.5	1580	21.6	1.5		244.0
HA-i5-4			50.0	10.0		59.0
HA-i5-5			21.4	1.8		60.0

Figure 4.2: Data from the characterization tests performed on the H-A well. The scheme of the well shows the formations of the seal-reservoir system and the depths to which such formations have been cut. To the right of the figure the length of the interval in each test sample is illustrated. The following test data are presented in the table: interval length (position of the upper and lower ends), overpressure produced during the test, flow rate, injection volume and injection time.

The tests were performed using a straddle packer system (Heavy Duty Double Packer System (HDDP). The system consists essentially of two tubing-deployed packers with an injection interval length of 28.80 m between the packers, a shut-in tool to close the hydraulic connection between the injection tubing and the injection interval, and three pressure sensors (Plw shows pressure values connected with the interval below the lower packer, Pin shows pressure values connected with the injection interval between the two packers

and Pup shows pressure values connected with the interval above the upper packer, whereas PAup show Upper PAcker pressure and PAlw shows Lower PAcker pressure) (Figure 4.3).

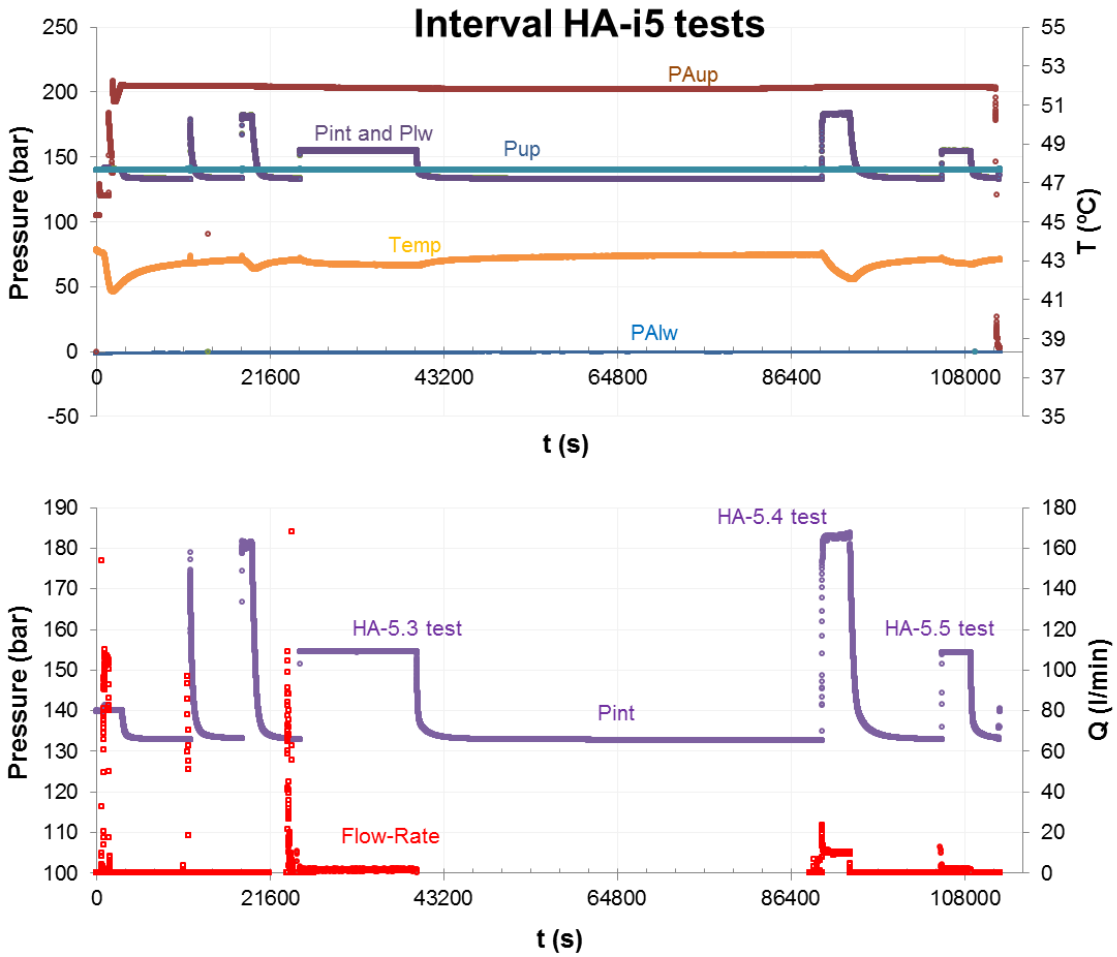

Figure 4.3: Data measured on the H-A well during the tests. The upper graph shows the measured pressure and temperature. Pint and Plw are identical because the lower packer is unset (PAlw = 0 bar). The lower graph shows the Q and Pint measurements. Legend: pressure at the tested interval (Pint); Plw: Pressure at Lower interval; Pup: Pressure at Upper interval; PAup: Upper PAcker pressure; PAlw: Lower PAcker pressure

4.2 HYDRAULIC TESTS ON H-I WELL

Several brine injection and recovery tests were carried out between November, 8th and 14th, 2013 in well H-I and the crosshole response was observed in well H-A. Based on the results of the first tests at H-A, rather than injecting in a portion of the aquifer thickness as shown in Figure 4.2, which led to low injection rates, it was decided to inject throughout the whole reservoir thickness. Therefore, tests in H-I were carried over the whole aquifer thickness.

The tests were performed by using a single packer system installed in the injection well H-I on November 10th and 11th (see Appendix 2). The system consists of a tubing-deployed TAM I.E. 139.7mm (5.5”) packer and a pressure and temperature memory gauge (Keller DCX-22) located below the packer. The tubing string is hydraulically connected to the interval below the packer. Two additional pressure gauges (Keller

PAA-33X) located at surface recorded the pressure in the injection string and the inflation pressure of the packer.

The single packer system installed in the observation well H-A on November 11th (see Appendix 1) consists of a winch-deployed TAM I.E. 128.52mm (5.06”) packer (fig. 4.4) and two pressure gauges (Keller PAA-33X) located in a Downhole Electronic Housing: one measures pressure in the interval below the packer and the other one measures the packer inflation pressure.

Figure 4.4: Winch used for characterization tests at Hontomin

In the control shed on site, an accelerometer was installed to register microseismic events; some seismic activity was noted during the hydraulic tests, but of very low magnitude comparable to natural background noise).

Figure 4.5 shows the tests data (pressure variation produced in each test, flow injection, extracted volume and duration of the injection) and a scheme of the well column detailing the formations and tested intervals.

Figure 4.6 shows the parameters measured during the tests, at both wells H-I (injection) and the H-A (observation).

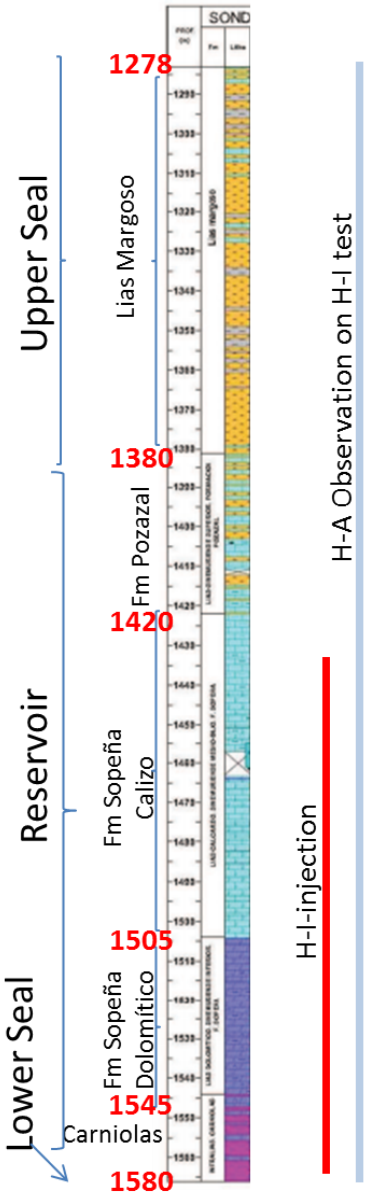

H-I Test

TEST	Interval Length (m)		DP (bar)	Q (l/min)	V_{Iny} (l)	t_{Iny} (min)
HI-Ri1	1436	1570	1.3	2.3	74.0	32.2
HI-Ri2	1436	1570	0.3	4.9	30.9	6.3
HI-Ri3	1436	1570	0.3	9.5	33.8	3.6
HI-Ri4	1436	1570	35.0	26.7	1363.4	51.0
HI-Ri5	1436	1570	2.9	39.1	645.6	16.5
HI-Ri6	1436	1570	10.8	55.8	1738.1	31.2
HI-Ri7	1436	1570	5.0	78.3	2385.7	30.5
HI-Ri8	1436	1570	3.0	100.7	3102.4	30.8
HI-Ri9	1436	1570	4.0	120.0	7298.0	60.7
HI-Ri10	1436	1570	18.5	117.6	7238.0	61.5
HI-Ri11	1436	1570	16.3	119.2	7324.5	61.5
HI-Ri12-1	1436	1570	5.6	60.0	3600	60.0
HI-Ri12-2	1436	1570	26.2	120	8027.0	66.0
HI-Ri12-3	1436	1570	31.0	180	10585.0	59.0

Figure 4.5: Data from the characterization tests performed on the H-I well. The scheme of the well shows the formations of the seal-reservoir system and the depths to which the formations have been cut. To the right of the figure the length of the interval in each test sample is shown. The following test data are presented in the table: interval length (position of the upper and lower ends), overpressure produced during the test, flow rate, injection volume and injection time.

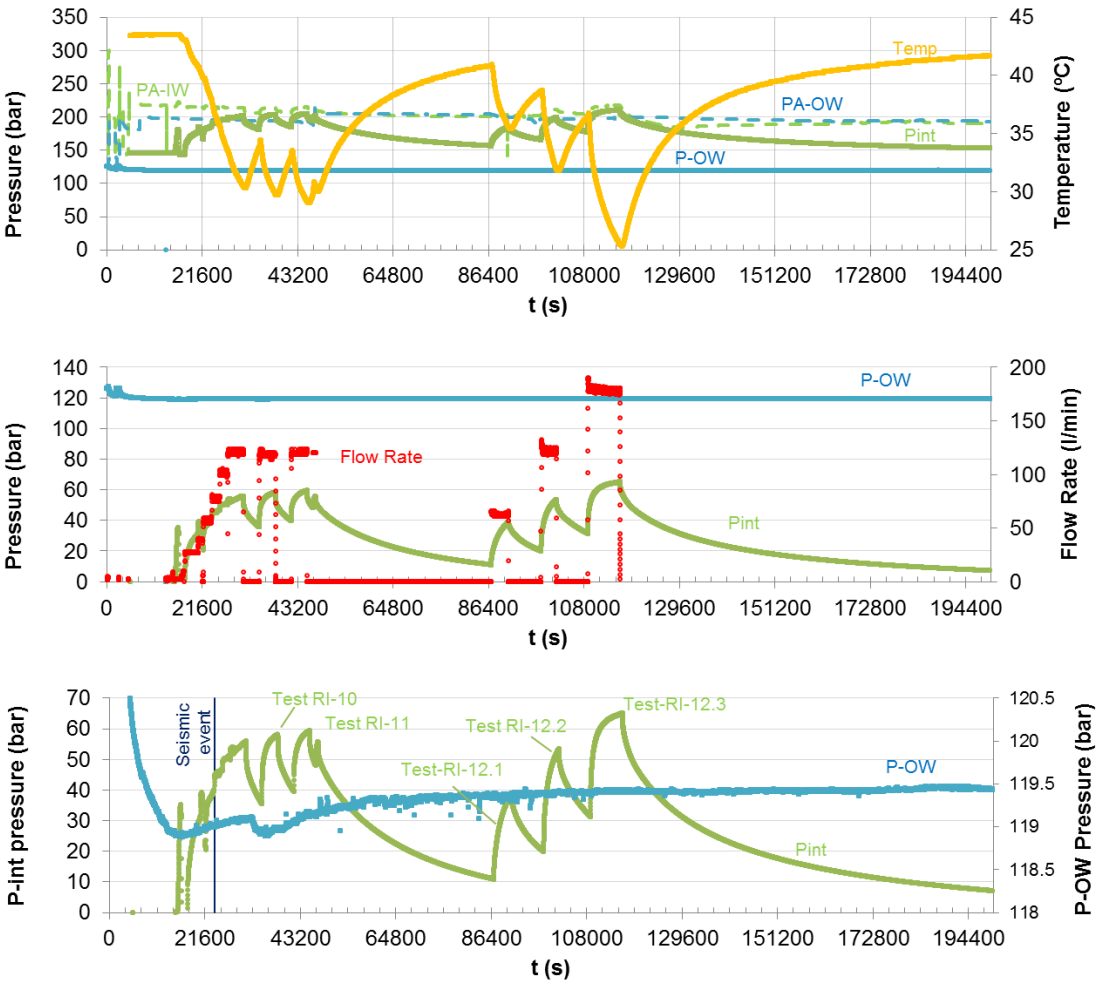

Figure 4.6: Data measured on the H-I well during the tests. Legend: packer pressure (PA-OW), pressure on the tested interval (Pint), and temperature (T); pressure recorded at the observation well (P-OW).

5 INTERPRETATION OF TEST DATA

The interpretation of the hydraulic tests has been made using the following steps:

i. Filtering and de-trending of the data, calculation of drawdowns

ii. Calibrating each test individually to obtain a first estimate of hydraulic parameters during each test phase.

iii. Interpretation of the complete series of hydraulic tests performed on each well using purely hydraulics models.

iv. Interpretation of the complete series of hydraulic tests performed on each well using hydro-mechanical models.

In this report we focus on the interpretation of individual tests results and complete series interpretation using different approaches.

5.1 CONVERSION OF UNITS

The interpretation methods used in this report yield hydraulic transmissivity values *T* (in m^2/d). In order to convert them into hydraulic conductivity *K* (in m/d), *T* was divided by the thickness of the formations open to the well (133m in H-I and 299m in H-A).

Hydraulic conductivity *K* (in m/d) was converted to intrinsic permeability *k* (in mD) according to equation (5.1):

$$k = K \frac{\mu}{\rho g} \frac{1[\mathrm{d}]}{86400[\mathrm{s}]} 10^{15} \left[\frac{\mathrm{mD}}{\mathrm{m}^2} \right] \tag{5.1}$$

Using a water density ρ = 1030 kg/m^3, a water viscosity μ = 0.00068 Pa·s at 40 °C and the gravity constant *g* = 9.81 m/s^2, the conversion factor is:

$$k[\mathrm{mD}] = \frac{K}{0.00128} \left[\frac{\mathrm{m}^2}{\mathrm{d}} \right] \tag{5.2}$$

5.2 INDIVIDUAL TEST RESULT INTERPRETATION

Each injection and its corresponding recovery were first interpreted using diagnostic plots.

To obtain the maximum information from the results, we represent pressure buildup in two different ways. Pressure buildup versus logarithm of time [*s vs log (t)*] and derivative of pressure buildup versus logarithm of time [*d(s) / d(log(t)) vs log(t)*]. In the first type of graphs, data should tend to form a straight line for large times if flow is radial (Cooper-Jacob approximation). Transmissivity can be obtained from the slope of this line, whilst the storage coefficient results from its intersection with the *log t* axis. The second representation uses the derivative of the pressure buildup with respect to *log (t)*, thereby yielding directly the slope, and thus the transmissivity. This type of representation is more sensitive to changes in hydraulic properties near the well, which facilitates identifying them. Detailed explanations on the method are provided by Bourdet et al. (1983) and Renard et al. (2009).

5.2.1 Analytical interpretation

The diagnostic plots of the injection period of the H-A test are not very informative, because flow rates were highly variable and pressures were only measured in the injection well and were therefore strongly influenced by skin and other well-effects. Recovery was interpreted using the Theis method and Agarwal's (1980) method (showed in this report). In both methods, periods with approximately constant derivative were used to calculate transmissivity from the slope.

In the Agarwal method (assuming that pumping or injection took place at an approximately constant rate), the recovery data points are transformed into Agarwal equivalent time t_A as:

$$t_A=t_p \cdot t'/(t_p+t')$$

where t_p is the duration of pumping [time units], and t' is time since pumping stopped [time units]. The residual pressure is calculated as:

$$s_A=s_p-s'$$

where s_A is recovery measured from s_p [length units], s_p is total drawdown at the end of pumping [length units], s' is residual drawdown during recovery [length units]. From these data the time derivatives can be calculated as explained above to construct a diagnostic plot.

Agarwal's method is a good option for early recovery times, but it is less accurate for later stages of tests. For later times it may be better to use the Theis recovery method. We illustrate both in the HI-12-3 test (Figure 5.1) recovery methods. The curves show that transmissivity decreases with time due to the closure of fracture net during the recovery period, showing a transition that to final transmissivity values at the end of the test, when the fracture network has closed. This is the value we adopt as the natural transmissivity value of the reservoir.

The values shown in the tables are obtained under the influence of the tests, and will depend on the pressure exerted on each test.

(a)

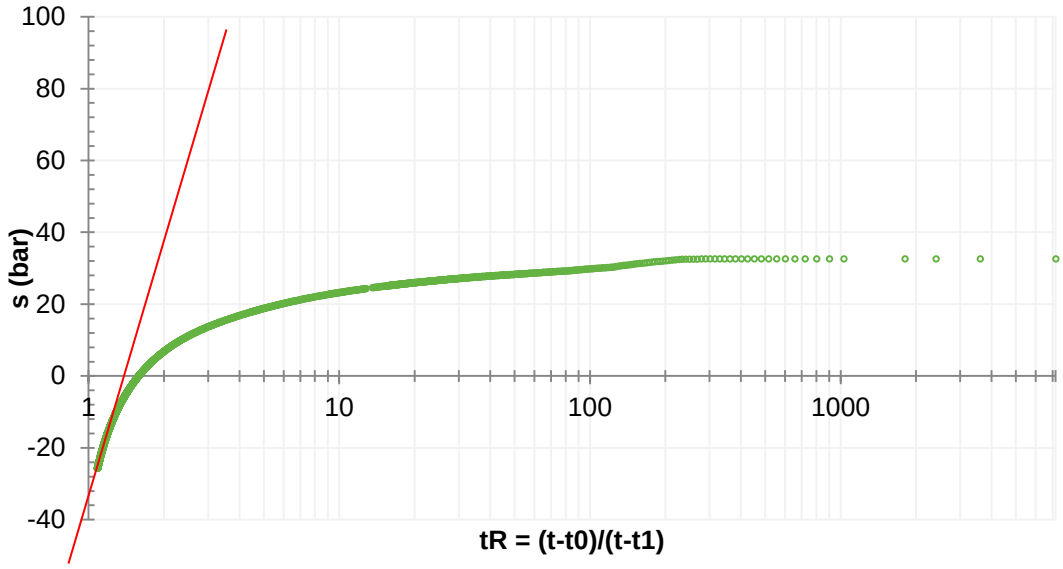

(b)

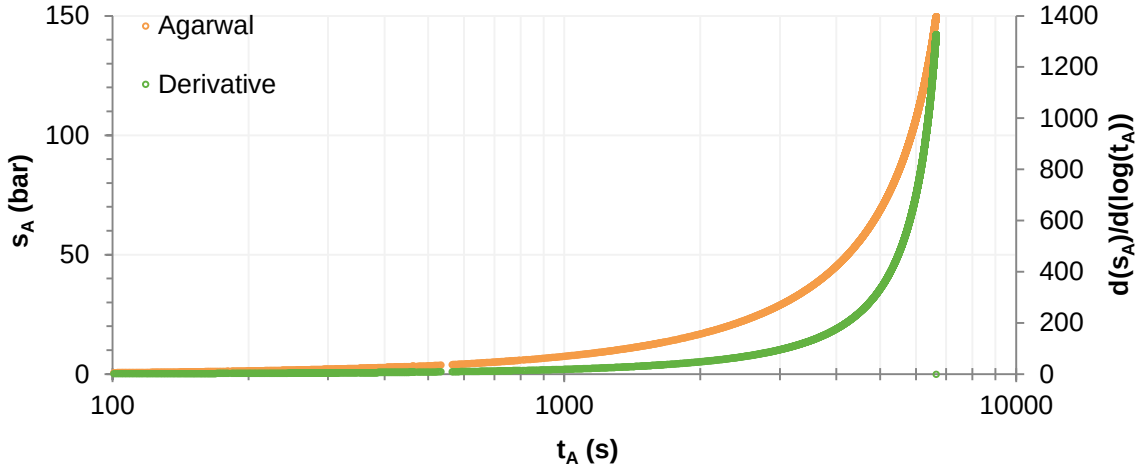

Figure 5.1: R12.3 tests interpretation using (a) Theis and (b) Agarwal (1980) recovery methods.

5.2.1.1 H-A tests (August 2013)

The three injection sets performed using a pump (tests 5.3, 5.4 and 5.5) were analysed. The injection plots are not very informative, but recovery plots of the three tests clearly show that pressure transients are greatly affected by wellbore storage and skin effects.

Table 5.1 summarizes the results obtained using this method.

Table 5.1: Slope m, injection rate Q and transmissivity estimated using Agarwal's method for the tests carried out in well H-A in August 2013.

Injection	m (bar)	m (m)	Q (l/min)	Q (m^3/d)	T (m^2/d)	k (mD)	T (mD*m)
5.3	5	50	1.5	2.16	0.0079	0.037	6.18
5.4	21	210	10	14.4	0.0126	0.059	9.81
5.5	5.5	55	1.8	2.592	0.0086	0.041	6.74

In test 5.3, a constant slope was observed between Agarwal time 500 sec and 2000 sec. approximately, with a slope of 5 bar per log cycle, indicating a transmissivity of about 0.008 m^2/day. The shape of the diagnostic plots of recoveries for 5.4 and 5.5 is similar and the slopes determined from the plots are indicative of transmissivity at a relatively large distance from the well. It is worth pointing out that the slope drops towards the end of all tests; this may reflect a significant increase in transmissivity at a large distance from the pumping well or flow towards a fracture from the matrix. This issue will be revisited in the next section.

5.2.1.2 H-I tests (November 2013)

Recovery plots show very untypical behaviour. Instead of approaching an asymptotic constant value, slopes in the Agarwal plots tend to increase during recovery, indicating that transmissivities were much lower during late recovery than at the beginning. This suggests that fractures opened due to the injection pressure generated in the well, and closed again when overpressure fell off during early recovery. However, the slope increase (i.e., indicating that estimated transmissivity decreases) during injection is contradictory. Another explanation would be a boundary effect (i.e that the H-I well would be located in an isolated compartment of the reservoir with a limited volume). As an example, the plots of test R12.3 are given in Figure 5.1.

The slopes and transmissivities determined by the Agarwal method are given below (

Table 5.2). A plateau in the slopes has been observed for relatively early Agarwal times, and represents the high transmissivities obtained at the beginning of recovery. These high transmissivities are located in the vicinity of well H-I, as opposed to well H-A, where the plateau in the slope was observed for later times of recovery (representing the transmissivity further away from H-A well).

This mixed behaviour indicates that:

i. Transmissivity in H-I is higher than in H-A,

ii. Estimated transmissivities increase with injection rate,

iii. The transmissivity response of the formation near H-I has a mechanical component (changing slopes in all the tests),

Table 5.2: Slope m, injection rate Q and transmissivity estimated using Agarwal's method for the tests carried out in well H-I in November 2013.

Interval	m (bar)	m (m)	Q (l/min)	Q (m3/d)	T(m2/d)	k (mD)	T (mD*m)
RI 10	19.5	195	116.6	167.9	0.158	0.93	123.10
RI 11	44.5	445	119.6	172.2	0.071	0.42	55.31
RI 12.1	44	440	61.6	88.7	0.037	0.22	28.81
RI 12.2	76	760	121.2	174.6	0.042	0.25	32.84
R1 12.3	125	1250	177.9	256.1	0.037	0.22	29.30

5.2.2 Numerical interpretation

This interpretation has been made using the test data of each injection individually. To perform this interpretation we assumed that the injected brine is pressurized at the well interval and flows into the aquifer and fractures. We have observed a low permeability zone around the well walls that has been represented as a skin effect (Figure 5.2). The model represents a 2D homogeneous media with a radial symmetry and horizontal radial flow. The thickness of the aquifer is 133 m for H-I and 165 m for H-A, the radius in both cases is 2000 m. The fracture has a radius of 50 m and a thickness of 5 cm.

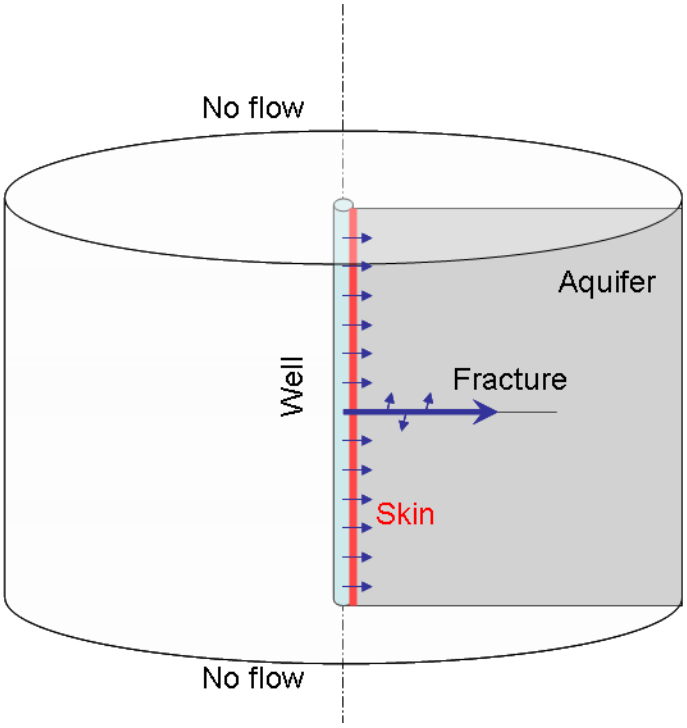

Figure 5.2: Conceptual model

5.2.2.1 H-A tests

In this well, recovery trends were completely different from the injection trends. The recovery plot displays two clearly identified slopes, on a semi-log plot. These slopes may reflect two zones with different hydraulic behaviour. Initially, pressure recovered faster (inner annulus of low transmissivity, which has been

represented as a 5 cm skin), reaching a moment when the pressure recovery was slower (higher T in the formation).

The obtained parameters are shown in Table 5.3. One of the obtained fits is shown on Figure 5.3.

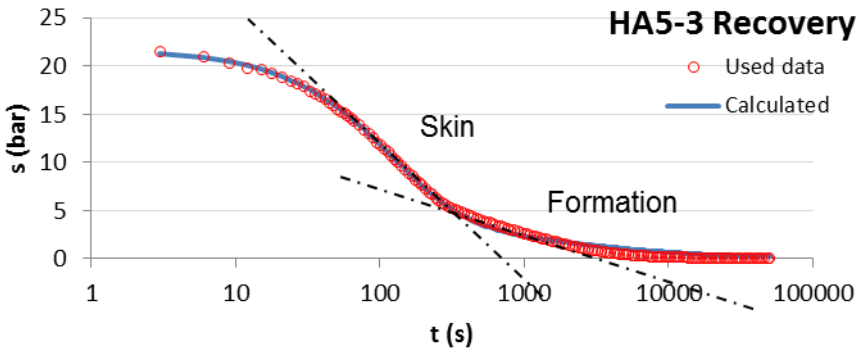

Figure 5.3: Hydraulic interpretation of the HA5-3 test

Table 5.3: Hydraulic parameters of the tests carried out in well H-A (HA-i5-3, 4 and 5 tests, see Error! eference source not found.) ranges of variation. Specific Storativity S_S (m^{-1}) is given for the aquifer and skin, Storativity S_F (-) is given for the Fracture.

H-A	T (m^2/d)	k (mD)	T (mD*m)	S_S (m^{-1}) or S_F (-)
Aquifer	1.6E-03 - 1.9E-02	7.4E-03 - 9.0E-02	1.2E+00 - 1.5E+01	1.8E-07 - 4.6E-06
Skin	7.6E-04 - 6.7E+00	3.6E-03 - 3.1E+01	5.9E-01 - 5.2E+03	1.8E-07 - 4.6E-06
Fracture	7.2E-03 - 2.2E-02		5.6E+00 - 1.7E+01	1.0E-08 - 1.0E-08
Well	1	4.73E+00	781.25	4.45E-06

Comparing the results of the interpretation of the H-A tests, it can be seen that the transmissivity had a large range of variation (Table 5.3). The transmissivity was greater with the higher flowrate injection (test 5.4). When the overpressure was higher, the fractures could have been opening more, thus increasing transmissivity.

5.2.2.2 H-I tests

The behavior of this well was completely different to that of the H-A test, as the buildups were not as sharp. A particular and notable feature of the H-I tests was their recovery trends (Figure 5.4); the injection and the early portion of the recovery data fitted with the same transmissivity values. Afterwards, the permeability seemed to decrease, yielding a recovery trend with a lower slope. Table 5.4 displays the hydraulic parameters obtained in the calibration of these tests (injection and recovery separately).

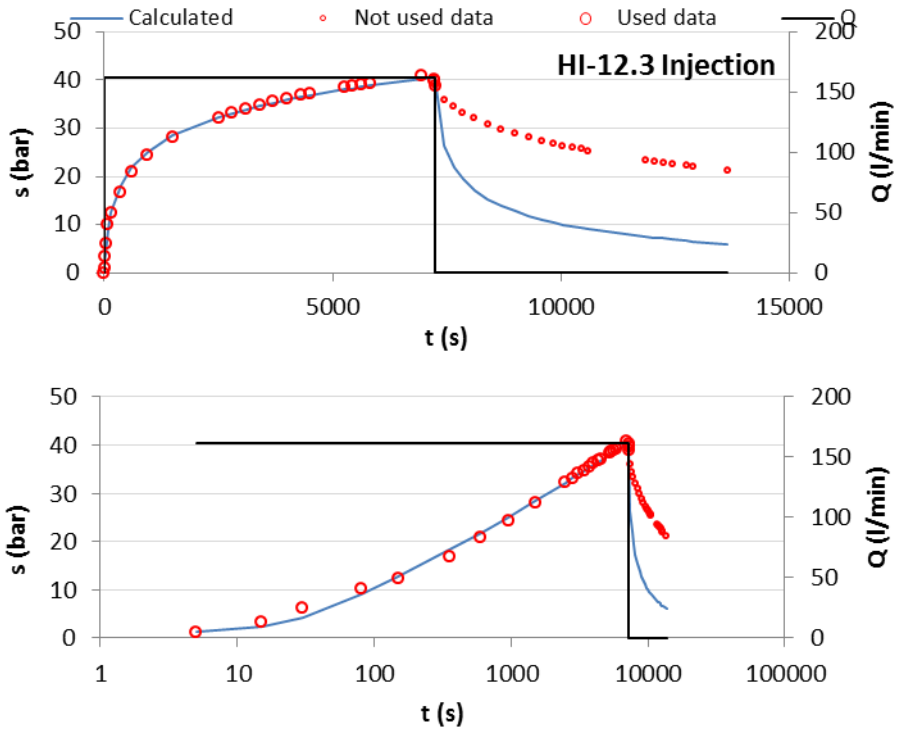

Figure 5.4: Hydraulic interpretation of the H-I-R12.3 test

Table 5.4: Hydraulic parameters of the tests carried out in well H-I (see **Figure**), ranges of variation during injection (inj.) and recovery (rec.). Specific Storativity S_S (m^{-1}) is given for the aquifer, Storativity S_F (-) is given for the Fracture.

HI-inj.	T (m^2/d)	k (mD)	T (mD*m)	S_S (m^{-1}) or S_F (-)
Aquifer	1.4E-02 - 2.3E-02	8.2E-02 - 1.4E-01	1.1E+01 - 1.8E+01	7.0E-04 - 1.0E-03
Fracture	1.0E-04 - 1.5E-03		7.8E-02 - 1.2E+00	1.0E-08 - 2.2E-07
Well	1	5.87E+00	781.25	4.45E-06

HI-rec.	T (m^2/d)	k (mD)	T (mD*m)	S_S (m^{-1}) or S_F (-)
Aquifer	1.3E-03 - 3.0E-03	7.6E-03 - 1.8E-02	1.0E+00 - 2.3E+00	4.0E-03 - 1.3E-02
Fracture	1.0E-04 - 2.8E-04		7.8E-02 - 2.2E-01	2.0E-07 - 2.2E-07
Well	1	5.87E+00	781.25	4.45E-06

Table 5.4 shows the ranges of variation of the calculated parameters in all tests interpretations. The values obtained in the interpretations of the injections are greater than those calculated for recoveries. This effect could be explained as the opening of the fracture networks due to the increase of pressure during the injection period. During the RI-11 injection period, the H-I borehole showed an increase in transmissivity -

probably the repeated injections removed residual drilling muds on the borehole walls. Accordingly, in the last tests 12.1 to 12.3 no skin effect was observed.

5.3 INTEGRATED NUMERICAL INTERPRETATION

Ideally, all test results should be fitted with the same model and the separate interpretation of the tests discussed in the previous chapter is not satisfactory. This chapter aims to fit all measured responses using a time-integrated numerical interpretation. This approach is advantageous in that it avoids the need for de-trending when the recovery period is short. We undertook this in two ways: firstly interpreting the tests with a single model (i.e. constant permeability) using the TRANSIN code, where the main differences with the interpretations of Section 5.2 are the filtering of raw data with interpretation highlighting the effect on build-up pressures of actual variations of transmissivity. Secondly use PROOST, which offers considerable flexibility in the parameterization of fields and time functions, and allows constant transmissivity values within each time interval (representing a test) to be adjusted.

The conceptual model is the same as before (Figure 5.2).

5.3.1 Hydraulic integrated numerical interpretation with TRANSIN

The TRANSIN code (Galarza et al., 1999) allows automatic calibration of flow and transport parameters. Parameters estimated during the analytical interpretation are used as initial values of the model parameters for calibration.

In this interpretation all measurements have the same weight (1), so the model tries to adjust all the measurements simultaneously.

5.3.1.1 HA tests on the whole interval (sequence HI-5.1 through 5)

Figure 5.5 shows the fits obtained with the parameters of Table 5.5; the model cannot fit all pressure changes due to the variations of hydraulic parameters. This may reflect the increase in permeability due to fracture opening. The HA5-4 test has a flow rate one order of magnitude greater than the HA5-3 and HA5-5 test, but the pressure does not vary in the same extent. Therefore a constant transmissivity cannot fit all the data. It is also worth noting that the pressure remained constant during the injection periods, which reflects an injection rate that was probably not constant.

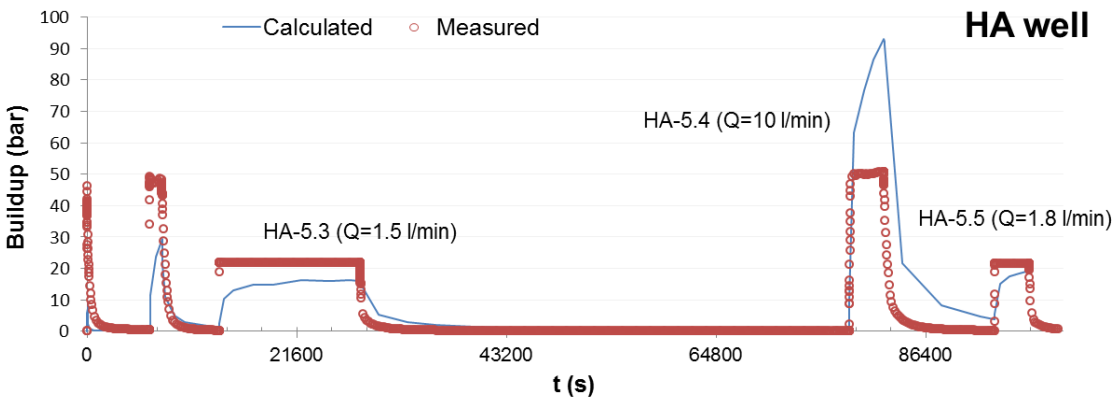

Figure 5.5: Observed and simulated (TRANSIN) well response to injection in the H-A well

Table 5.5: Calibrated model parameters of the integrated H-A test. Specific Storativity S_S (m^{-1}) is given for the aquifer and skin, Storativity S_F (-) is given for the Fracture.

HA	T (m^2/d)	k (mD)	T (mD*m)	S_S (m^{-1}) or S_F (-)
Aquifer	0.011	0.05	8.59	4.00E-07
Skin	0.003	0.01	2.06	4.00E-07
Fracture	0.072		56.25	2.00E-08
Well	72	340.91	56250	4.45E-06

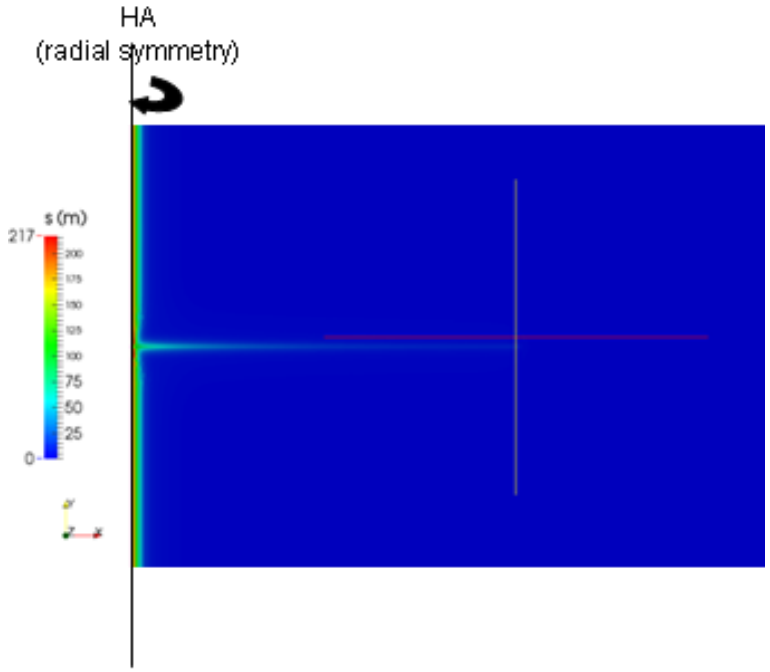

Figure 5.6: Drawdown calculated on the H-A tests. See the fracture effect (drawdowns are represented in m).

Figure 5.6 displays the drawdown calculated at the end of one of the injections in the H-A tests. The picture shows the skin effect, limiting the increase of pressure to the well vicinity, and the fracture.

5.3.1.2 H-I tests

Figure 5.7 represents the measured (dots) and calculated (line) pressure at the H-I tests (parameters in Table 5.6). As has been discussed before, it is not possible to reproduce the build-ups and the recoveries with the same hydraulic parameters.

The H-I model needs a more transmissive and compressible aquifer than the H-A test. The effect of the skin seems to be necessary at the beginning of the test, but diminishes with time. This effect prevents adjustment of the initial rise of test H-I.

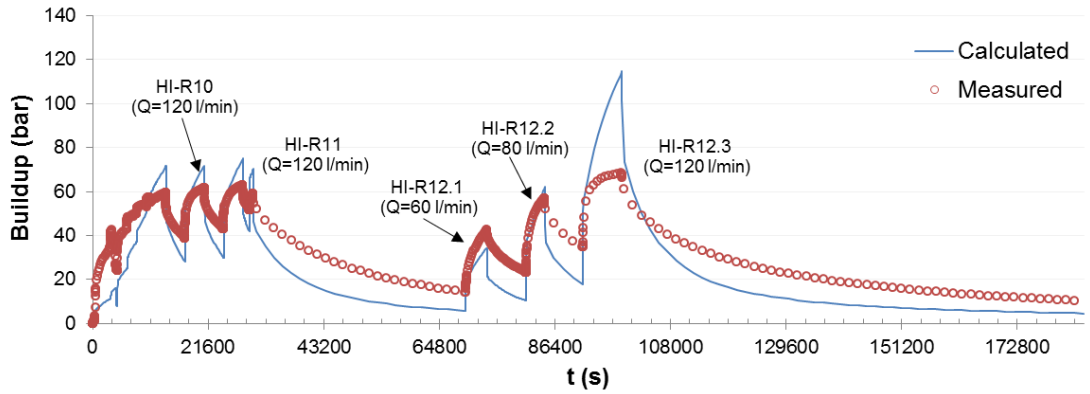

Figure 5.7: Observed and simulated with constant parameters (TRANSIN) well response to injection in the H-I well.

Table 5.6: Calibrated model parameters of the integrated H-I test. Specific Storativity S_S (m^{-1}) is given for the aquifer, Storativity S_F (-) is given for the Fracture.

HI	T (m^2/d)	k (mD)	T (mD*m)	S_S (m^{-1}) or S_F (-)
Aquifer	0.097	0.6	76.1	3.70E-05
Fracture	0.432		337.5	2.00E-08
Well	1	5.9	781.25	4.45E-06

5.3.2 Integrated numerical interpretation with PROOST

The calibration with TRANSIN described in Section 5.3 is not satisfactory. For example, in the case of the H-A well (

Figure **5.5**), the simulated response to the injection is below the observed response in all cases, except for the response to the injection HA-5.4 at the highest flow rate. This suggests that the hydraulic properties of the system changed during the injection tests, which is consistent with the spread of parameters obtained from the interpretations of each injection and recovery period.

Therefore, we have used the program "PROOST" (Slooten et al., 2010) to test this alternative hypothesis: that the aquifer and/or fracture properties changed in time due to mechanical effects. This could occur because the increased groundwater pressure could force fractures open, or have led to deformation of the porous matrix. In particular, we assumed that there would be a difference in the transmissivity during injection and recovery periods.

To test this idea, we optimized transmissivity parameters for each injection and recovery period. Parameters were chosen as a function of the injection time-series. Every time the pump was switched on or off, a new transmissivity parameter was introduced.

5.3.2.1 Interpretation of H-A

After analysing the optimal parameters found by TRANSIN for the H-A injection tests (Table 5.5) we fixed storativity and fracture permeability throughout the domain, and calibrated the transmissivity of the formation and the skin (Table 5.7). Time-dependent parameterization for transmissivity was used as discussed above for each injection and recovery period of the five tests (see Figure 5.8). The parameters were assumed to be statistically independent, and no prior information was used.

Table 5.7: The fixed parameters in the calibration of the H-A well response. Specific Storativity S_S (m^{-1}) is given for the aquifer and skin, Storativity S_F (-) is given for the Fracture.

	T (m^2/d)	k (mD)	T (mD*m)	S_S (m^{-1}) or S_F (-)
Aquifer	0.003 - 0.284	0.020 - 1.669	2.61 - 222	4.69E-07
Skin	0.068	0.402	53.497	4.69E-07
Fracture	0.023 - 5.274		17.6 - 4120	2.35E-08
Well	68.480	402.26	53500	4.00E-06

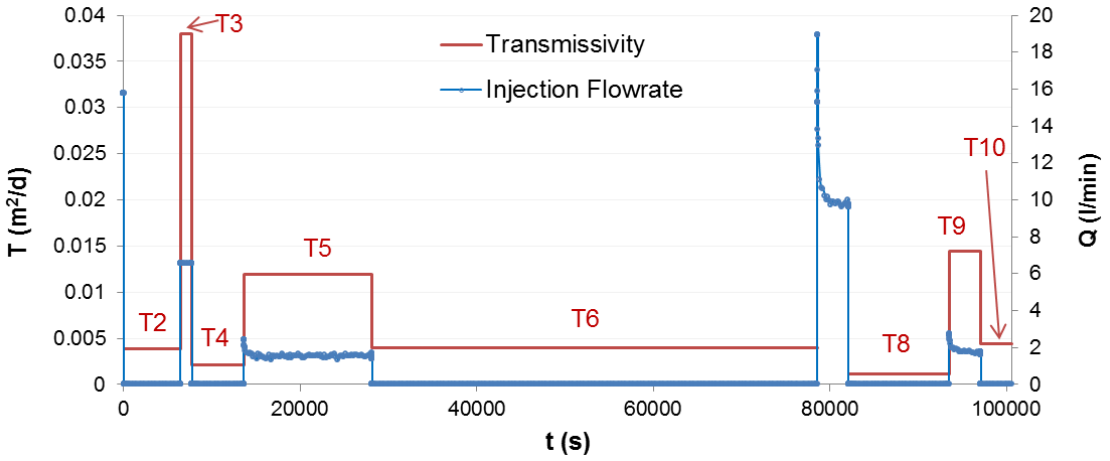

Figure 5.8: The injection flowrate (blue), and transmissivity values (red) used during the different injection and recovery periods of H-A.

The following parameters were obtained in the calibration (Table 5.8):

Table 5.8: The calibrated parameters from H-A well response, transmissivities of the injection periods are shaded in grey.

	T (m^2/d)	k (mD)	T (mD*m)	Description
Skin	0.003	1.25E-02	2.059	
T1	20.849	9.87E+01	16288.0	Injection 5.1
T2	0.004	1.85E-02	3.053	Recovery 5.1
T3	0.038	1.80E-01	29.673	Injection 5.2
T4	0.002	1.00E-02	1.651	Recovery 5.2
T5	0.012	5.66E-02	9.344	Injection 5.3
T6	0.004	1.88E-02	3.106	Recovery 5.3
T7	4696.574	2.22E+04	3669198.8	Injection 5.4
T8	0.001	5.51E-03	0.909	Recovery 5.4
T9	0.014	6.83E-02	11.269	Injection 5.5
T10	0.004	2.08E-02	3.433	Recovery 5.5

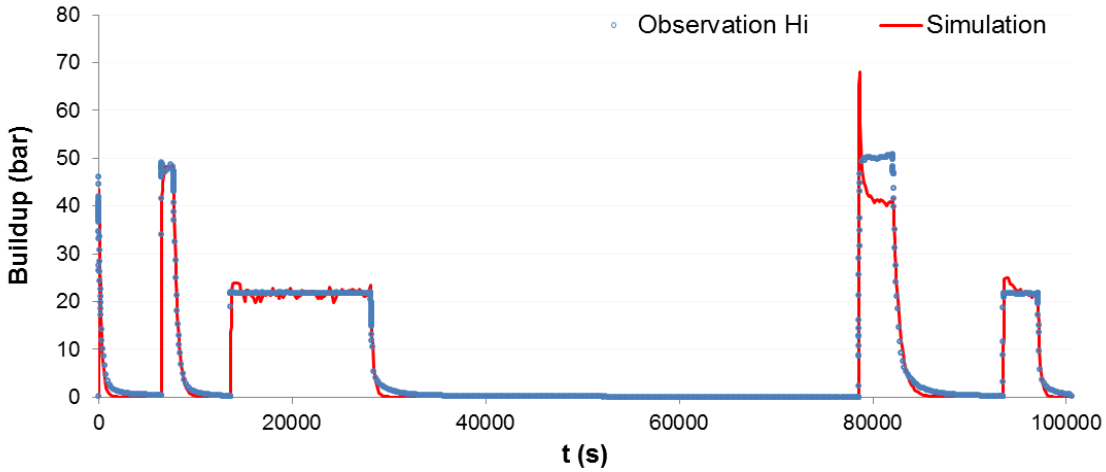

Figure 5.9: Final fit between observations and simulated values in H-A.

Figure 5.9 shows that the fits obtained for the H-A hydraulic tests improved considerably. The estimated parameters seem reasonable except for T1 and T7, which are too high. In the case of T1, this is probably due to the fact that during this injection (5.1), no pump or flowmeter were used. Instead, the wellhead was pressurized with nitrogen gas, and the flow rate was inferred from head differences which may have induced large errors. Moreover, T1 was estimated using sparse data. In the case of T7, the very high transmissivity may be an artefact of the optimization methodology caused by the large peak in flow rate at the beginning of injection 5.4. Due to these flow data, the model produced a start peak in the computed build-up values followed by a plateau, while the observations only showed a plateau. In order to minimize the objective function, the optimization algorithm has put the simulated plateau below the observed data and the peak above it. For the simulated plateau to lie below the observed one, a very high transmissivity would be needed - far higher than that of even the most permeable gravels. Consequently, T7 results are disregarded.

Once T1 and T7 are removed, recovery and injection parameters can be compared (Figure 5.10; Table 5.8). It can be seen that the recovery parameters are similar to each other and are all below the smallest injection parameter. Injection transmissivities display more variation; this could indicate dependence on injection rate or on pressure, which would explain why different injection experiments yield different parameters. In general, the results support our hypothesis that the transmissivity is different during injection and recovery. In Section 0 the possible relation between pressure and transmissivity is further explored from a geomechanical point of view.

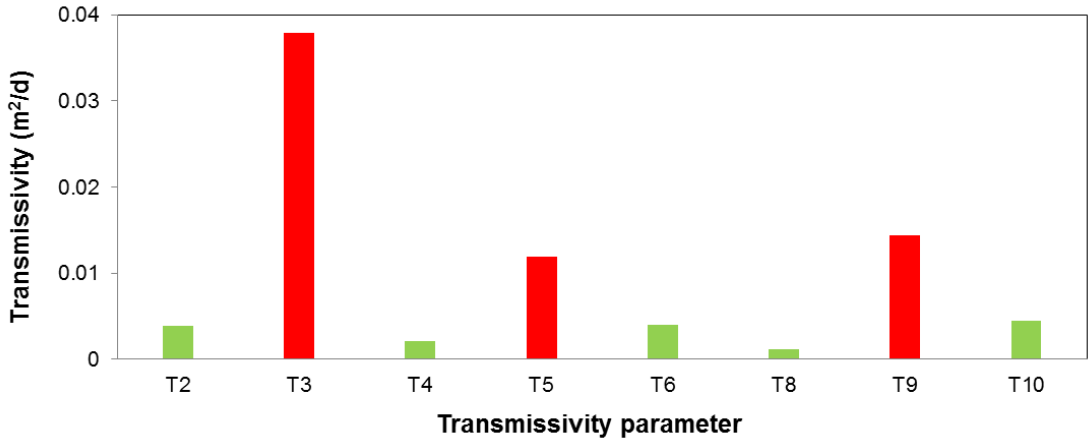

Figure 5.10: The transmissivity parameters obtained using PROOST in H-A. Those corresponding to injection periods are shown in red, those corresponding to recovery in green. The unrealistic parameters T1 and T7 are discarded.

5.3.2.2 Interpretation of H-I

After a first calibration was made in TRANSIN (Figure 5.7), a time dependent parameter model was attempted to verify the change of properties between the different injection periods. In all numerical simulations, the transmissivity of the fracture and the matrix were time-varying as most sensitive parameters. Other parameters were assumed as constant.

Although the hydraulic conductivity of a fracture is time-varying, this has not been calibrated due to its high conductivity; instead, the calibrated parameter has been the hydraulic conductivity of the aquifer. The other parameters have been maintained.

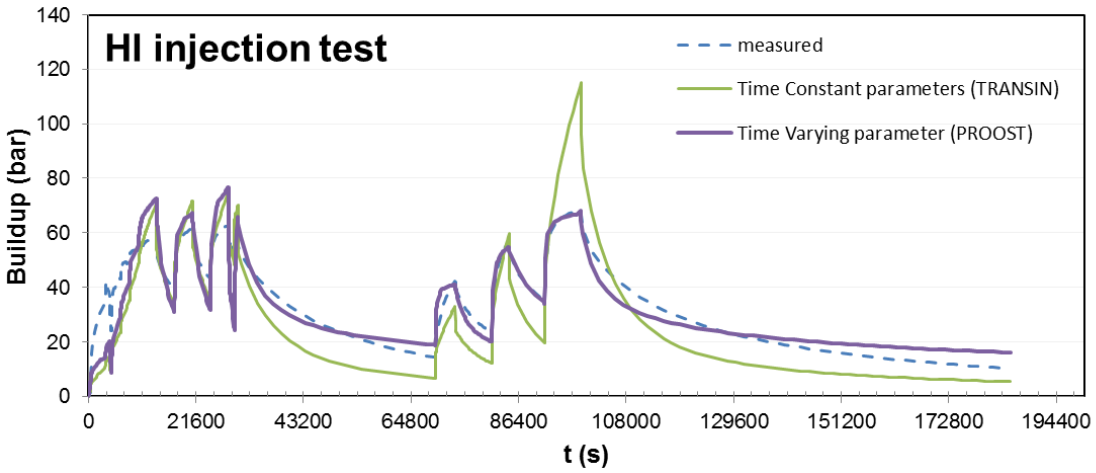

Figure 5.11: Evolution of the measured and simulated build-up and recovery in H-I injection test

Although the results do not fit the observations exactly (Figure 5.11), PROOST can adjust the build-up and the recovery curves better for the whole field test than TRANSIN. We can conclude that the physical properties of our aquifer varied according to flowrate.

The comparison between transmissivity obtained with evolution of the fracture and the aquifer matrix; and injection flow is shown in Figure 5.12.

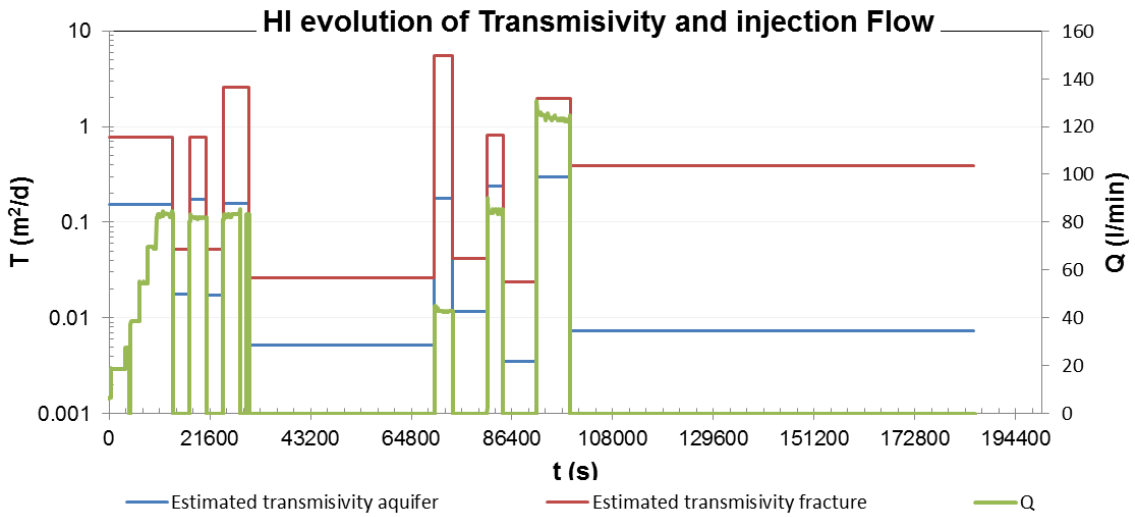

Figure 5.12: Time evolution of the fracture and aquifer transmissivity and flowrate in H-I

The parameter ranges obtained from the H-I injection tests are shown in Table 5.9:

Table 5.9: Estimated transmissivity and storage coefficients of the different model zones for well H-I using PROOST. Specific Storativity S_S (m^{-1}) is given for the aquifer and skin, Storativity S_F (-) is given for the Fracture.

	T (m^2/d)	k (mD)	T (mD*m)	S_S (m^{-1}) or S_F (-)
Aquifer	0.003 - 0.284	0.020 - 1.669	2.61 - 222	4.69E-07
Skin	0.068	0.402	53.497	4.69E-07
Fracture	0.023 - 5.274		17.6 - 4120	2.35E-08
Well	68.480	402.26	53500	4.00E-06

The last three injections (HI-12.1 to HI-12.3) yielded transmissivity values for the aquifer that increased consistently with overpressure (Figure 5.13), providing an estimate of the hydro-mechanic behavior of the aquifer during injections with different overpressures and flow rates.

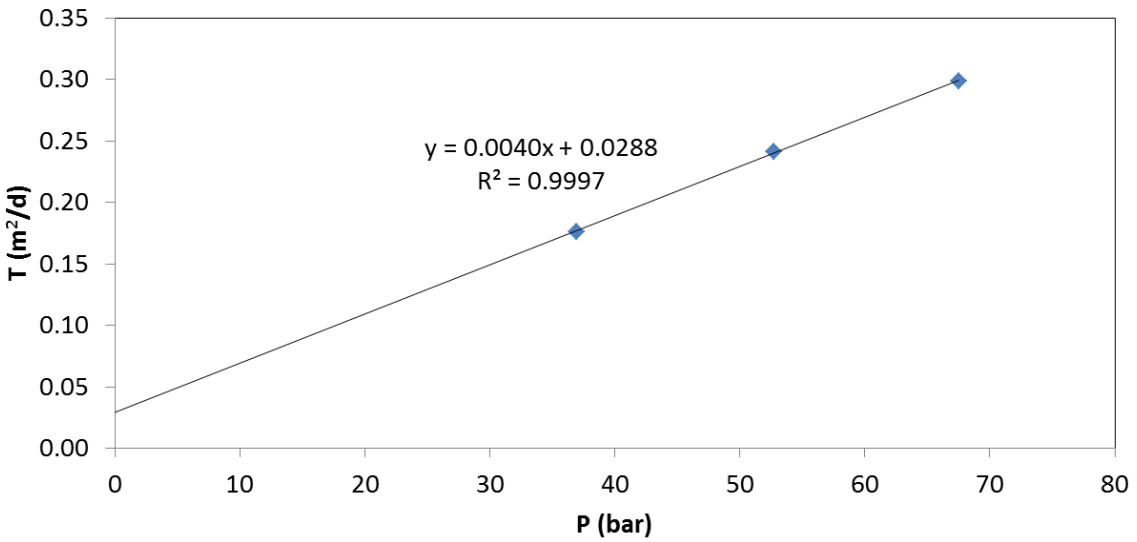

Figure 5.13: Variation of transmissivity values with pressure increase during hydraulic tests HI12-1 to HI-12.3 in well H-I.

Hydro-mechanic integrated numerical interpretation

The above interpretations demonstrate the aquifer response to be highly non-linear (i.e. no constant transmissivity), possibly reflects coupled mechanical effects which are further investigated in the section below.

5.3.3 Introduction and motivation

Hydro-mechanical (HM) coupling refers to the mutual interactions between hydraulic and mechanical processes. Water pressure influences stresses and strains and is in turn influenced by the latter, which may also change porosity and thus intrinsic permeability. Pressure increases serve to decrease effective stresses, which may cause deformation. Hence pressure changes can alter porosity, leading to a variation of aquifer storage capacity and in some cases to a change of intrinsic permeability. In fractured reservoirs the increase of overpressure and consequent reduction of the effective stresses, may increase fracture apertures or even induce shear failure. The former mechanism is generally elastic and leads to an increase of intrinsic permeability related to the aperture size, which is reversible if overpressure is recovered; the latter mechanism is plastic and leads to an increase of intrinsic permeability related to the joint asperity (dilatancy) that is irreversible if overpressure is recovered. The sliding activation is usually associated with seismic activity of small magnitude. Increases of intrinsic permeability may exceed 2 orders of magnitude. In both porous and fractured medium, the variations of hydraulic conductivity lead to a significant coupling between flow and pressure variations.

Hydraulic models with constant intrinsic permeability were not able to reproduce the pressure behavior during entire injection tests (see Section 5.3). In the H-A test, the increase in flow rate injection did not correspond to the increase in overpressure. This means that intrinsic permeability changed during the injection, so it is likely that changes in fracture aperture and/or sliding was activated. The same behavior was observed in the H-I test, where a rapid decrease in pressure was recorded during the RI-6 test (time 172 min); the latter can be explained only with a sudden shear failure of a fracture. This assumption is supported by micro- seismicity recorded during the H-I tests.

Hydro-mechanic (HM) simulations of the injection tests were performed, taking into account the variations of reservoir transmissivity. It should be noted that the aim of the HM simulations in this document is to explain the general behavior of the aquifer during the injection tests, not provide a quantitative calibration.

It is also worth noting that thermal effects may be involved in the process, as the injected water was cooler with respect to the deep reservoir. Temperature variations affect stress directly because of thermal contraction, but also indirectly because water flux is related to temperature by density and viscosity. Nevertheless and for the sake of simplicity, thermal effects have not been introduced in the simulations so far.

5.3.4 Methods

The same geometry of hydraulic models as in Sections 5.3 has been used, adding a caprock layer. The mechanical properties (Young Modulus *E*, Poisson ratio *v*) and permeability of the caprock have been obtained from an average of sample analysis results. An isotropic medium has been assumed. Values are shown in Table 5.10; transmissivity of the reservoir and of the fracture have been calibrated with trial and error methods, in order to fit the observed overpressure.

Table 5.10: Parameters considered in the reference case for HM simulations

	k (mD)	***E*** (MPa)	***v*** (-)
Caprock	0.001	30000	0.3
Reservoir	-	30000	0.3
Fracture	-	20000	0.3

A permeability variation law has been adopted to account for variations during the injection tests. In fractured media the intrinsic permeability k depends on fracture aperture b, according to the cubic law $k = \frac{b^3}{12}$ (Fig. 5.14). As the fracture aperture increases with increasing liquid pressures, permeability will change according to the cube of the aperture variation. We consider that permeability changes in an elastic manner with variations of fracture aperture, although sliding is provoked if rupture conditions are reached.

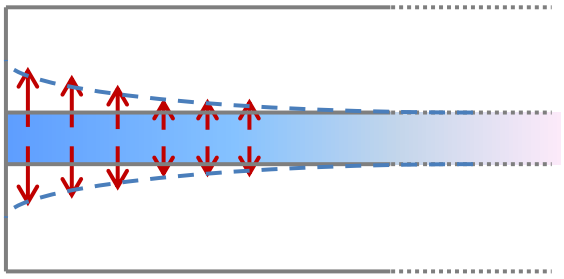

Figure 5.14: Schematic representation of the fracture aperture increase with increasing pressure

Skin effects were neglected and initial reservoir transmissivity was considered constant, although a complex system of fractures and fissures is likely to cause spatial variations of transmissivity.

Considering both hydro-mechanical coupling and the deformation permeability law, reservoir transmissivity and fracture initial transmissivity were varied in order to fit modelled overpressure to experimental data.

Simulations have been carried out with the finite element code CODE-BRIGHT (Olivella et al., 1996) that allows hydro-mechanical (HM) simulations.

5.3.5 Results

5.3.5.1 H-A injection test

The best fit between observations and simulation (Figure 5.15) has been achieved using a value of 0.01mD (which corresponds to a transmissivitiy of 0.002m^2/d) for the reservoir permeability and of 0.03mD (which corresponds to a transmissivity of 0.005m^2/d) for the fracture initial permeability (see Table 5.11). With increasing overpressure, the fracture opens and transmissivity changes. This implies that temporal variations are not uniform in space: close to the well, where overpressure and deformations are greater, permeability reaches a maximum value of about 0.38mD (which corresponds to a transmissivity of 0.064m^2/d) (Figure 5.16). Figure 5.17 shows the values of transmissivity of the fracture versus distance from the well for 3 different times. Note that the appearance of this figure is similar to that of the aperture, illustrating that the fracture opens around the well and that the opening is relatively uniform.

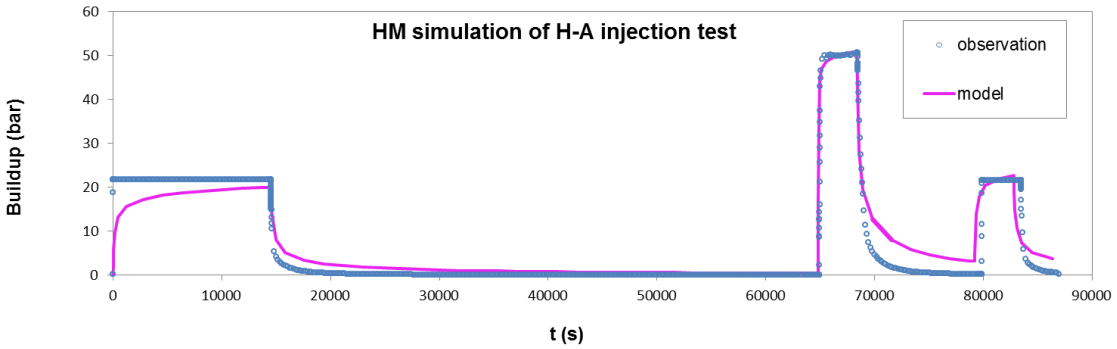

Figure 5.15: Variation of overpressure in the well. Observed vs simulated data

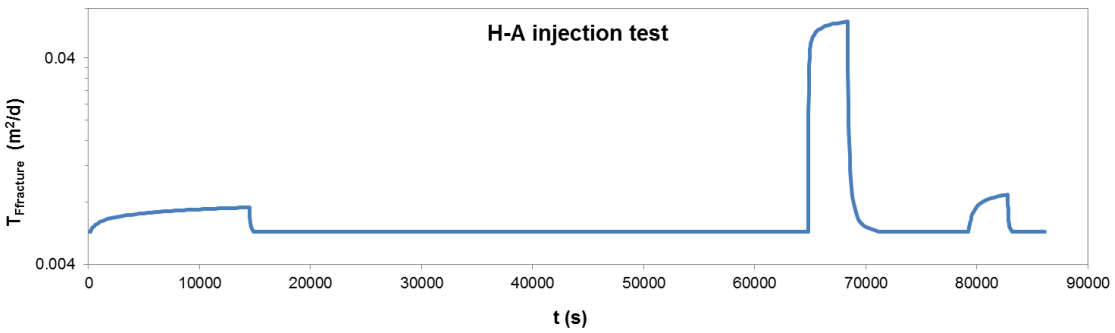

Figure 5.16: Temporal evolution of fracture transmissivity for a point placed close to the well

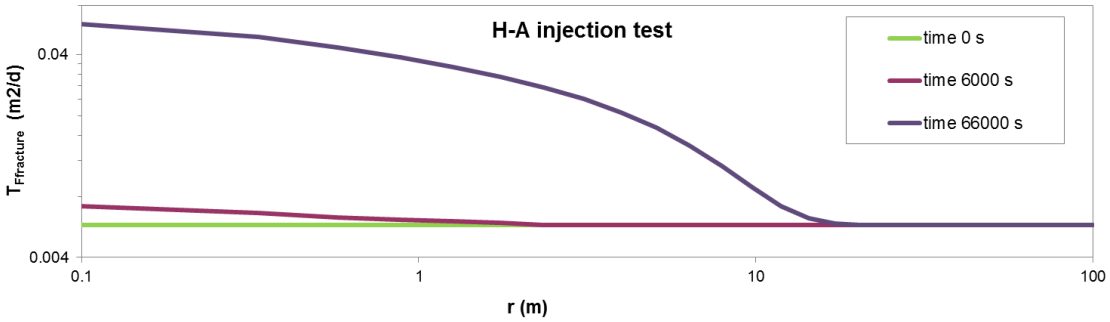

Figure 5.17: Transmissivity of fracture versus distance from injection well for times 0, 100 and 1,100 mins

Table 5.11: H-A parameters obtained in the HM model

HA well	T (m^2/d)	k (mD)	T (mD·m)	S (m^{-1})
Aquifer	0.002	0.01	1.5	4.70E-07
Fracture	0.005 - 0.05	0.03 - 0.27	4.5 - 44	9.50E-07
Well	1.28E+07	6.06E+07	1.00E+10	7.00E-06

5.3.5.2 H-I injection test

The best fit between observations and simulations (Figure 5.18) was achieved assuming a value of 0.01mD (which corresponds to a transmissivity of 0.002m^2/d) for the reservoir permeability and of 0.38mD (which corresponds to a transmissivity of 0.064m^2/d) for the fracture initial permeability (see Table 5.12).

As for H-A injection test, the transmissivity variation in time is not uniform in space: close to the well, where overpressure and deformations are greater, permeability reaches a maximum value of 6 mD (which corresponds to a transmissivity of 1.2 m^2/d) (Figure 5.19). Figure 5.20 shows the values of fracture transmissivity versus distance from the well for 3 different times.

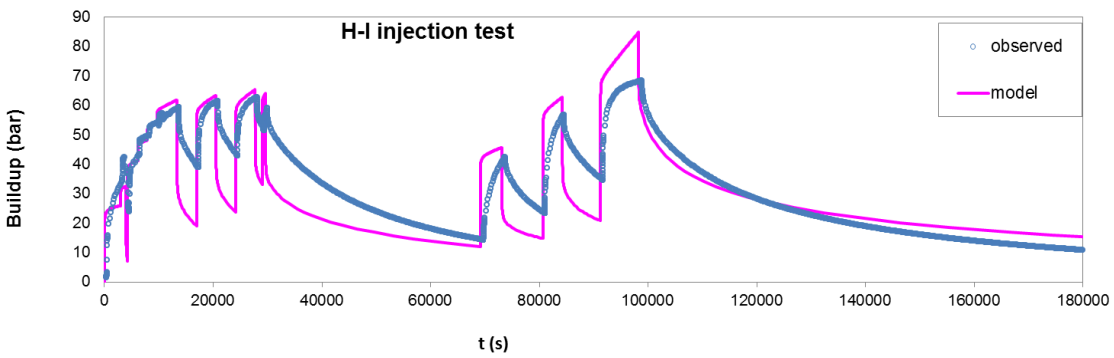

Figure 5.18: Variation of overpressure in the well. Observed vs simulated data

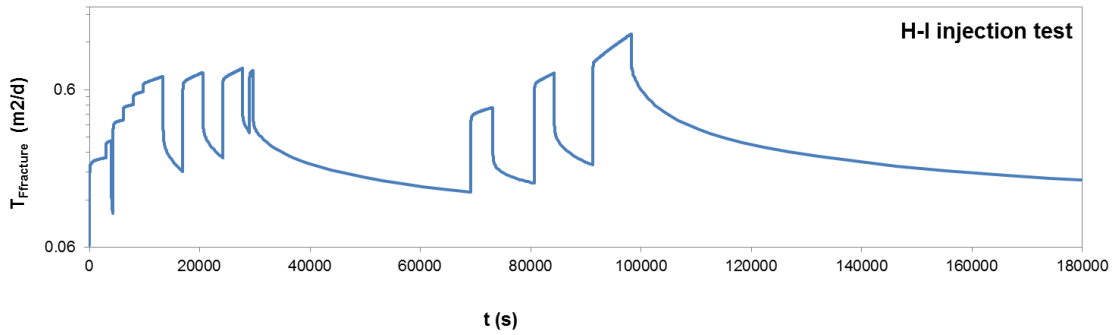

Figure 5.19: Temporal evolution of transmissivity for a point placed close to the well

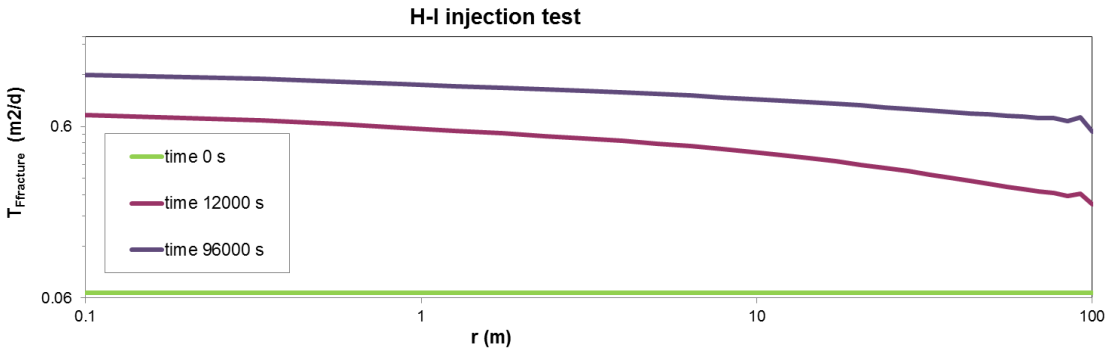

Figure 5.20: Fracture transmissivity vs distance from injection well for times 0, 200 and 1600 min.

Table 5.12: H-I parameters obtained in the HM model

HI well	T (m^2/d)	k (mD)	T (mD·m)	S (m^{-1})
Aquifer	0.002	0.01	1.5	4.70E-07
Fracture	0.064 - 1.19	0.38 - 7.01	50 - 932	9.50E-07
Well	1.28E+07	7.52E+07	1.00E+10	7.00E-06

For this simulation it was difficult to achieve a good fit between model and observations, especially in the first stage (70 mins) of the injection and in the recovery phase. Regarding the former, it is possible that in addition to elastic opening of the fracture, sliding was activated but has not been simulated. Regarding the latter, the discrepancy could be explained by the sudden stop of injection provoking a release of overpressure in the fracture with consequent and instantaneous closure of aperture. In this way transmissivity could reduce significantly whilst overpressures do not completely recover. In the model,

gradual increases in aperture are well simulated, in contrast to sudden decreases. To test this hypothesis other simulations should be performed, possibly using more complex conceptual models.

The HM coupling can explain reservoir behavior and the simulations can reproduce general overpressure trends. Better results could be obtained by considering more complex conceptual models, which falls beyond the objective of this report.

5.3.6 Summary of interpretative sections

When fluid is injected into a fractured storage formation, the increase of overpressure reduces the effective stresses acting normal to the fracture edges, leading to an increase of fracture aperture. This produces an elastic (reversible) increase of fracture transmissivity.

As overpressure depends on storage formation transmissivity which is pressure-dependent, the flow process that results is highly non-linear.

As fracture apertures increase with increasing liquid pressure, transmissivity will change according to the cube of the aperture variation and may increase by more than 2 orders of magnitude. Thus, injection in fractured storage formations is strongly affected by fracture responses to overpressure. Fracture aperture variation depends on stiffness and deformation characteristics. Deformation may also be inhibited by surrounding rock matrix stiffness. Furthermore, other parameters including injected flow rate and initial fracture transmissivity may be relevant.

It is therefore necessary to understand which factors govern this process. Due to the high non-linearity of the process, dimensionless analysis is problematic; in this study, a sensitivity analysis was based on numerical simulations of the H-I injection test. The assumed geometry comprised a horizontal fracture embedded in the middle of the storage formation with thickness of 130m, overlain by a caprock with a thickness of 200m. The model extends laterally 2,000m and is axisymmetric. Unlike the model used for the calibration, in this analysis the fracture has a 2,000m radius in order to avoid local effects and linear elastic behavior is assumed. Water is injected through a vertical well at a flow rate of 2L/s over 1h. Moreover, 4 hours of recovery are simulated after injection. Some parameters are considered constant, while others are the subject of sensitivity analyses. Parameters of the “base scenario” are shown inTable 5.13.

Table 5.13: Parameters of the “base scenario”

	k (mD)	E (MPa)	v (-)
Caprock (200 m)	0.001	30000	0.3
Storage formation (130 m)	0.01	30000	0.3
Fracture (0.5 m)	10 (k_0)	1000	0.3

It has been assumed that fracture intrinsic permeability changes according to the law $k = k_0 + \frac{(a \cdot \varepsilon)^3}{12a}$, where k_0 is fracture initial permeability, a is fractures spacing (assumed equal to 0.5m) and ε is deformation. This law considers an equivalent permeability for the fractured zone $k = k_0 + \frac{b^3}{12a}$ (which is in according

with the intrinsic permeability expression for fractures) and that the fracture aperture *b* is function of the deformation ε.

Sensitivity analysis was carried out considering fracture stiffness, storage formation stiffness, flow rate and initial fracture permeability or aperture.

The sensitivity analysis has shown that the most crucial parameter affecting induced overpressure is fracture stiffness - stiffer fractures are less able to deform. This results in a lower capacity to accumulate water and a slighter variation of intrinsic permeability; both issues lead to higher values of overpressure for stiffer fractures. Conversely, the penetration distance affected by overpressure and permeability variations, is almost the same for different values of fracture stiffness. Simulations with different fracture stiffness assumptions exhibit analogous behavior, although the relation between maximum pressure build-up and Young modulus is non-linear. An exponential dependence of pressure build-up on stiffness has been identified.

Regarding storage formation stiffness and initial fracture permeability, results of sensitivity analyses are very similar and indicate that these parameters do not significantly affect the process. However, it is possible that softer storage formations provoke lower overpressures, as expansion of fractures is less restricted.

Flow rate does not appear to have a significant effect on overall behavior. Fracture apertures and thus permeability are governed by the volume of injected fluid.

In summary, fracture stiffness is the parameter that most controls overpressure and permeability variations. It is unclear which parameter(s) affect the penetration distance, other than injection rate.

6 CONCLUSIONS

Hydraulic parameters of the fractured carbonate reservoir at Hontomin are different during the test injection and subsequent recovery periods. This observation may reflect the fracture network opening during the injection period because of the increase in pressure. During recovery periods, pressure decreases lead to closing of fractures.

Models assuming constant parameters over time are not able to reproduce this effect.

Estimates of transmissivity during injection were found to be consistently higher than those calculated for recovery periods. This mechanical effect was simulated using Hydro-Mechanical models (HM). From the results, attempts were made to determine the evolution of transmissivity in response to water injection. Although the observed data did not exactly fit these simulations, the exercise provided a qualitative behavioral correlation.

There appears to be a discrepancy between the values of parameters resulting from HM simulations and the ones obtained in hydraulic simulations of Section 5.3. This is because hydraulic simulations only consider temporal transmissivity variations. In the HM simulations, the variations of transmissivity depend on deformation and thus on overpressure. Therefore, the transmissivity will change only in the portion of the fracture affected by a certain level of overpressure, in turn related to the proximity of the well. Therefore the parameters estimated by the hydraulic simulations have to be considered as the equivalent of homogeneous fractures.

The dependence of transmissivity on the injection regime will be important in subsequent characterization tests, CO_2 experiments and modeling efforts. For design purposes and based on the works showed in this report, we propose the following values:

In well HA, transmissivity varied between 0.003m^2/d (which corresponds to a permeability of 0.015mD for the formation thickness of 165m) at low pressures and 0.04m^2/d (which corresponds to a permeability of 0.19mD) at high pressures. The well displayed a significant skin effect.

In well HI, transmissivity varied between 0.02m^2/d (which corresponds to a permeability of 0.12mD for the formation thickness of 133m) at low pressures and 0.3m^2/d (or 1.8mD) at high pressures (flow rate of 3L/s, and overpressure of 70bar at the well head). The well displayed some skin effect during the first injections, but this diminished with time.

Further characterization tests have been carried out in Hontomin, leading to a notable increase in permeability values in the reservoir. This underlines the need for extensive characterization of CO_2 storage sites in order to acquire a better understanding of the processes that will take place during the operational phase. Results from these tests will be taken into account in future reports involving Hontomin TDP operations.

7 BIBLIOGRAPHY

Agarwal, R.G., (1980). A new method to account for producing time effects when drawdown type curves are used to analyze pressure buildup and other test data. Society of Petroleum Engineers. Doi:10.2118/9289-MS.

Alcalde, J.; Marzán, I.; Saura, E.; Martí, D.; Ayarza, P.; Juhlin, C.; Pérez-Estaún, A.; Carbonell, R. (2014). 3D geological characterization of the Hontomín CO2 storage site, Spain:Multidisciplinary approach from seismic, well-log and regional data, Tectonophysics (2014), http://dx.doi.org/10.1016/j.tecto.2014.04.025

Bourdet, D., Whittle, T.M., Douglas, A.A., Pirard, Y.M., (1983). A new set of type curves simplifies well test analysis. World Oil 196, 95-106.

CO2CRC, 2008. Storage Capacity Estimation, Site Selection and Characterization for CO_2 Storage Projects. Cooperative Research Centre for Greenhouse Gas Technologies, Camberra. CO2CRC Report No: RPT08-1001. 52pp.

Cook, P J, 2006. Site Characterization. *In*: *International Symposium on Site Characterization for CO_2 Geological Storage*, 20-22 March 2006, Berkeley, California, USA. Lawrence Berkeley National Laboratory (LBNL), pp. 3-5.

Galarza, G., J.Carrera and A.Medina (1999). Computational techniques for optimization of problems involving non-linear transient simulations. *Int. J. Numer. Meth. Engng.* **45**: 319-334.

Olivella, S., Gens, A., Carrera, J. and Alonso, E. E. (1996) Numerical formulation for a simulator (CODE_BRIGHT) for the coupled analysis of saline media. *Engineering Computations*, 13 (7), 87-112.

Renard, P., Glenz, D., Mejias, M., 2009. Understanding diagnostic plots for well-test interpretation. Hydrogeology Journal 17, 589-600.

Slooten, L. J., Batlle, F. and Carrera, J. (2010). An XML based problem solving environment for hydrological problems. In Carrera, J. (ed.): *XVIII International Conference on Water Resources CMWR 2010*, CIMNE, Barcelona, 316-323.

Wildgust, N., Tontiwachwuthikul, P. And Gilboy, C (Eds) (2013). The IEAGHG Weyburn-Midale Monitoring and Storage Project. International Journal of Greenhouse Gas Control, Volume 16 Supplement 1, 308pp.

APPENDIX 1. INSTALLATION RECORD OF THE SOLEXPERTS HEAVY DUTY DOUBLE PACKER SYSTEM (HDDP) USED IN WELL HA IN AUGUST 2013

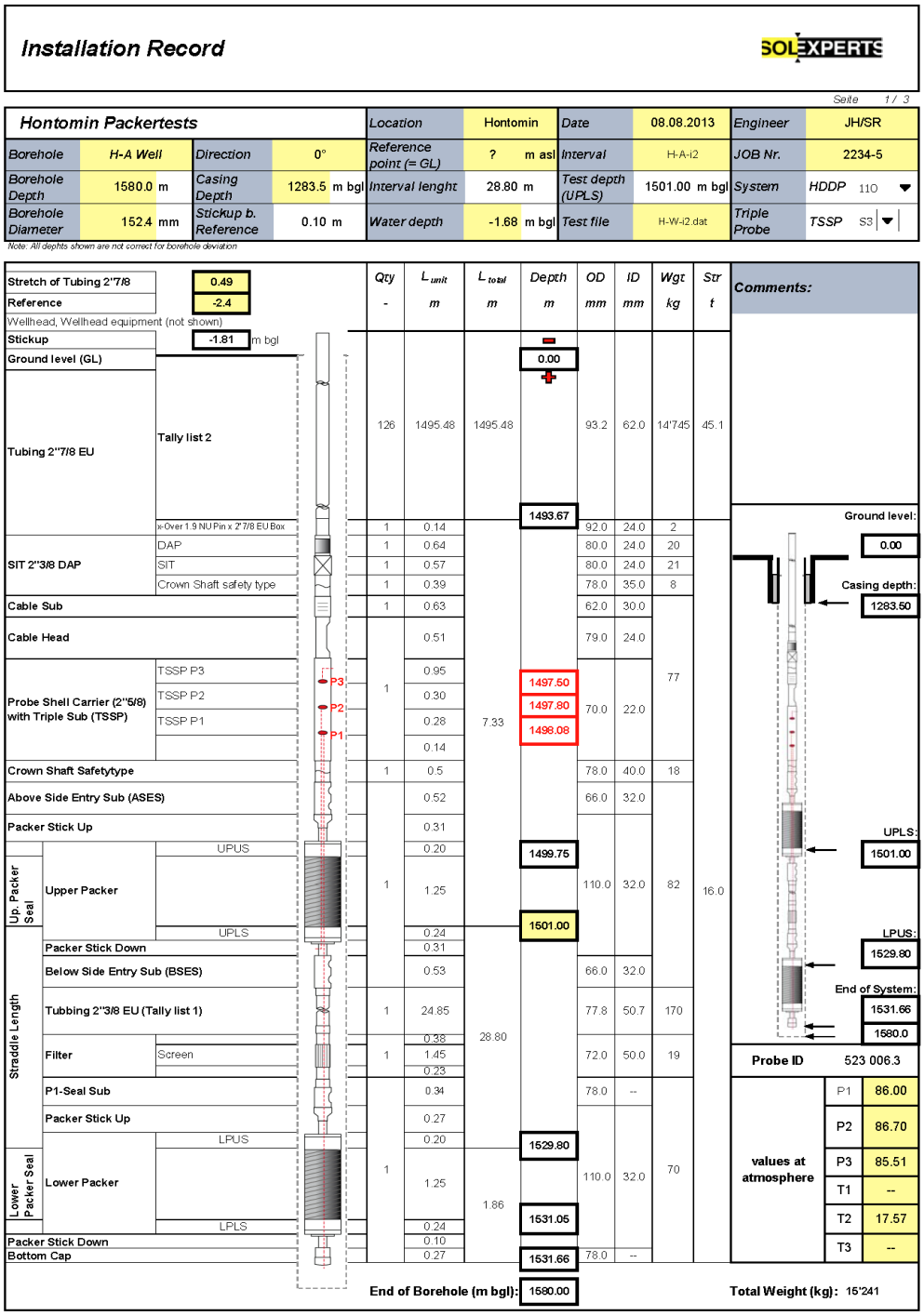

Installation Record — SOLEXPERTS

Seite 1 / 3

Hontomin Packertests				Location	Hontomin	Date	08.08.2013	Engineer	JH/SR
Borehole	H-A Well	Direction	0°	Reference point (= GL)	? m asl	Interval	H-A-i2	JOB Nr.	2234-5
Borehole Depth	1580.0 m	Casing Depth	1283.5 m bgl	Interval lenght	28.80 m	Test depth (UPLS)	1501.00 m bgl	System	HDDP 110
Borehole Diameter	152.4 mm	Stickup b. Reference	0.10 m	Water depth	-1.68 m bgl	Test file	H-W-i2.dat	Triple Probe	TSSP S3

Note: All depths shown are not correct for borehole deviation

		Qty -	L_{unit} m	L_{total} m	Depth m	OD mm	ID mm	Wgt kg	Str t
Stretch of Tubing 2"7/8	0.49								
Reference	-2.4								
Wellhead, Wellhead equipment (not shown)									
Stickup	-1.81 m bgl								
Ground level (GL)					0.00				
Tubing 2"7/8 EU	Tally list 2	126	1495.48	1495.48		93.2	62.0	14'745	45.1
					1493.67				
	x-Over 1.9 NU Pin x 2"7/8 EU Box	1	0.14			92.0	24.0	2	
SIT 2"3/8 DAP	DAP	1	0.64			80.0	24.0	20	
	SIT	1	0.57			80.0	24.0	21	
	Crown Shaft safety type	1	0.39			78.0	35.0	8	
Cable Sub		1	0.63			62.0	30.0		
Cable Head			0.51			79.0	24.0		
Probe Shell Carrier (2"5/8) with Triple Sub (TSSP)	TSSP P3	1	0.95		1497.50	70.0	22.0	77	
	TSSP P2		0.30		1497.80				
	TSSP P1		0.28	7.33	1498.08				
			0.14						
Crown Shaft Safetytype		1	0.5			78.0	40.0	18	
Above Side Entry Sub (ASES)			0.52			66.0	32.0		
Packer Stick Up			0.31						
Up. Packer Seal — Upper Packer	UPUS		0.20		1499.75				
		1	1.25			110.0	32.0	82	16.0
	UPLS		0.24		1501.00				
Straddle Length — Packer Stick Down			0.31						
Below Side Entry Sub (BSES)			0.53			66.0	32.0		
Tubbing 2"3/8 EU (Tally list 1)		1	24.85			77.8	50.7	170	
			0.38	28.80					
Filter	Screen	1	1.45			72.0	50.0	19	
			0.23						
P1-Seal Sub			0.34			78.0	--		
Packer Stick Up			0.27						
Lower Packer Seal — Lower Packer	LPUS		0.20		1529.80				
		1	1.25			110.0	32.0	70	
				1.86	1531.05				
	LPLS		0.24						
Packer Stick Down			0.10						
Bottom Cap			0.27		1531.66	78.0	--		
				End of Borehole (m bgl):	1580.00			Total Weight (kg):	15'241

Comments:

Ground level: 0.00

Casing depth: 1283.50

UPLS: 1501.00

LPUS: 1529.80

End of System: 1531.66

1580.0

Probe ID 523 006.3

values at atmosphere	
P1	86.00
P2	86.70
P3	85.51
T1	--
T2	17.57
T3	--

Figure A.1: Installation record of the Solexpert HDDP system used in well HA in August 2013

APPENDIX 2. INSTALLATION RECORD OF THE SOLEXPERTS PERFRAC-140 SYSTEM USED IN WELL HI IN NOVEMBER 2013

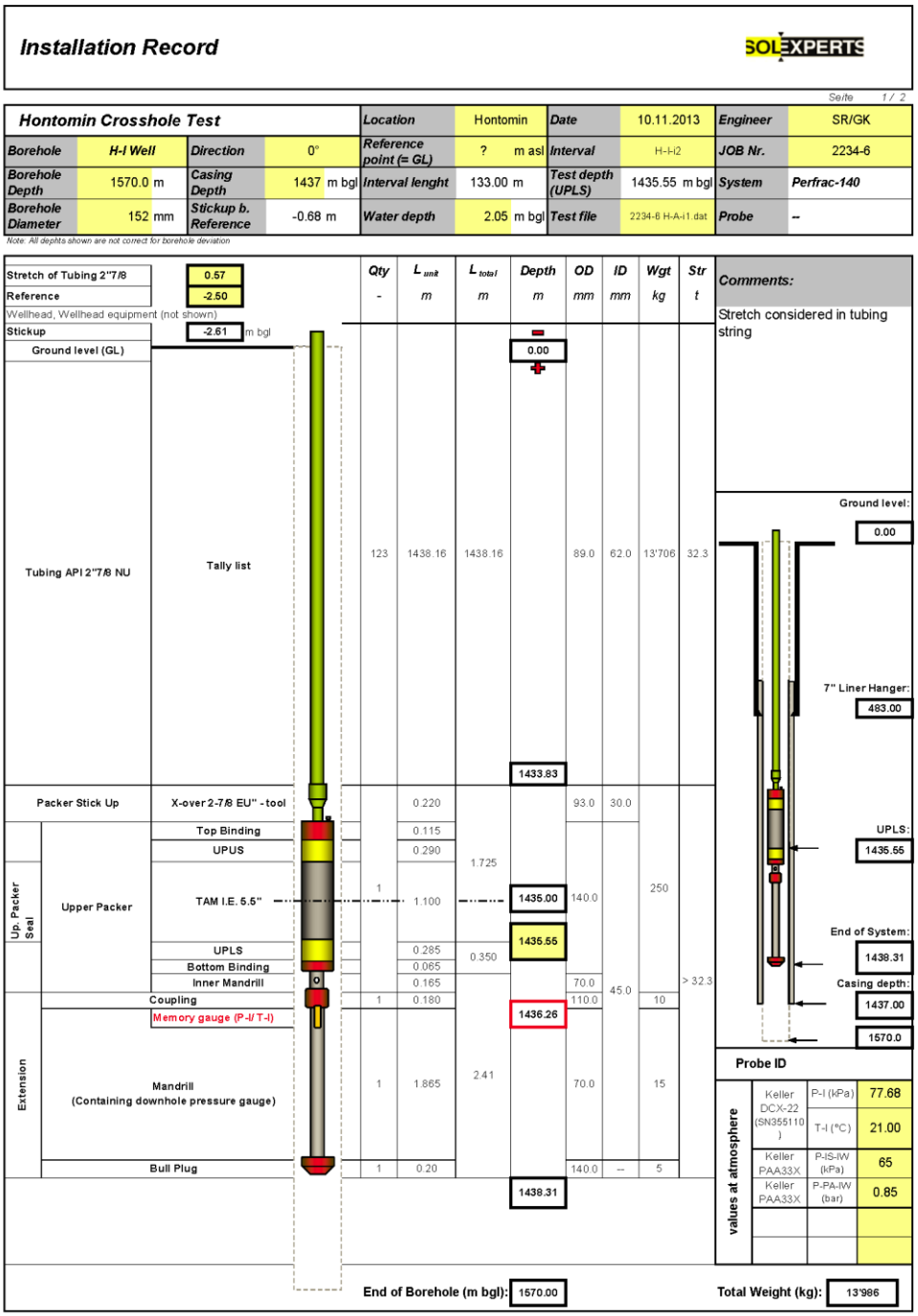

Installation Record

SOLEXPERTS

Seite 1 / 2

Hontomin Crosshole Test				Location	Hontomin	Date	10.11.2013	Engineer	SR/GK
Borehole	H-I Well	Direction	0°	Reference point (= GL)	? m asl	Interval	H-Hi2	JOB Nr.	2234-6
Borehole Depth	1570.0 m	Casing Depth	1437 m bgl	Interval lenght	133.00 m	Test depth (UPLS)	1435.55 m bgl	System	Perfrac-140
Borehole Diameter	152 mm	Stickup b. Reference	-0.68 m	Water depth	2.05 m bgl	Test file	2234-8 H-A-i1.dat	Probe	--

Note: All depths shown are not correct for borehole deviation

		Qty	L_{unit}	L_{total}	Depth	OD	ID	Wgt	Str
		-	m	m	m	mm	mm	kg	t
Stretch of Tubing 2"7/8	0.57								
Reference	-2.50								
Wellhead, Wellhead equipment (not shown)									
Stickup	-2.61 m bgl								
Ground level (GL)					0.00				
Tubing API 2"7/8 NU	Tally list	123	1438.16	1438.16		89.0	62.0	13'706	32.3
					1433.83				
Packer Stick Up	X-over 2-7/8 EU" - tool		0.220			93.0	30.0		
Up Packer Seal / Upper Packer	Top Binding		0.115						
	UPUS		0.290	1.725					
	TAM I.E. 5.5"	1	1.100		1435.00	140.0		250	
					1435.55				
	UPLS		0.285	0.350					
	Bottom Binding		0.065						
	Inner Mandrill		0.165			70.0	45.0		> 32.3
	Coupling	1	0.180			110.0		10	
Extension	Memory gauge (P-I/ T-I)				1436.26				
	Mandrill (Containing downhole pressure gauge)	1	1.865	2.41		70.0		15	
	Bull Plug	1	0.20			140.0	--	5	
					1438.31				

Comments:

Stretch considered in tubing string

Ground level: 0.00

7" Liner Hanger: 483.00

UPLS: 1435.55

End of System: 1438.31

Casing depth: 1437.00

1570.0

Probe ID

values at atmosphere		
Keller DCX-22 (SN355110)	P-I (kPa)	77.68
	T-I (°C)	21.00
Keller PAA33X	P-IS-IW (kPa)	65
Keller PAA33X	P-PA-IW (bar)	0.85

End of Borehole (m bgl): 1570.00

Total Weight (kg): 13'986

Figure A.2: Installation record of the Solexpert Perfrac-140 System used in well HI in November 2013